https://doi.org/10.5194/egusphere-2024-160
Preprint. Discussion started: 6 February 2024

A numerical model for duricrust formation by water table fluctuations

Caroline Fenske[1,2], Jean Braun[1,2], François Guillocheau[3], and Cécile Robin[3]

[1]German Research Centre for Geosciences GFZ, Helmholtz Centre Potsdam, Telegrafenberg, 14473 Potsdam
[2]Institute of Geosciences, University of Potsdam, Potsdam, Germany
[3]Université Rennes 1, Géosciences Rennes, 35042 Rennes

Correspondence: Caroline Fenske (fenske@gfz-potsdam.de), Jean Braun (braun@gfz-potsdam.de), François Guillocheau (francois.guillocheau@univ-rennes1.fr), Cécile Robin (cecile.robin@univ-rennes1.fr)

Abstract.

Duricrusts are hard elemental layers forming in climatically contrasted environments. Ferricretes (or iron duricrusts) are a type of duricrust, made of indurated iron layers. They form in tropical to semi-arid environments, but can be currently observed all around the world, in areas such as Africa, South America, India, and Australia. In most cases, they cap hills and appear to protect softer layers beneath. Two hypotheses have been proposed for the formation of duricrusts, i.e., the hydrological or horizontal model where the enrichment in the hardening element (iron for ferricretes) is the product of leaching and precipitation through the beating of the water table during contrasted seasonal cycles, and the laterisation or vertical model, where the formation of iron duricrusts is the final stage of laterisation.

In this article, we present the first numerical model for the formation of iron duricrusts based on the hydrological hypothesis. The model is an extension to an existing regolith formation model where the position of the water table is used to predict the formation of a hardened layer at a rate set by a characteristic time scale τ and over a depth set by the beating range of the water table, λ. Hardening causes a decrease in surface erodibility, which we introduce in the model as a dimensionless factor κ that multiplies the surface transport coefficient of the model.

Using the model we show under which circumstances duricrusts form by introducing two dimensionless numbers that combine the model parameters (λ and τ) as well as parameters representing external forcing like precipitation rate and uplift rate. We demonstrate that by using model parameter values obtained by independent constraints from field observations, hydrology and geochronology, the model predictions reproduce the observed conditions for duricrust formation. We also show that there exists a strong feedback from duricrust formation on the shape of the regolith and the position of the water table. Finally we demonstrate that the commonly accepted view that, because they are commonly found at the top of hills, duricrusts protect elements of the landscape is most likely an over-interpretation and that caution must be taken before using duricrusts as markers of uplift and/or base level falls.

https://doi.org/10.5194/egusphere-2024-160
Preprint. Discussion started: 6 February 2024

1 Introduction

Understanding Earth's surface evolution in cratonic areas remains difficult in parts due to its slow and therefore difficultly measurable rates but also due to the important contribution from chemical weathering and the formation of the regolith. Although some progress has been made recently in developing quantitative models of regolith formation and evolution on geological time scales (Lebedeva et al., 2010; Braun et al., 2016, 2017), many questions remain open, in part relating to the relative erodability (or resistance to physical erosion) of the weathering process products (Pelletier, 2010; Sacek et al., 2019). In particular, the formation of hard duricrusts is thought to protect the underlying softer weathered rock (Tardy, 1993; Taylor and Eggleton, 2001).

The term duricrust encompasses a broad range of hardened layers such as e.g. ferricretes, calcretes, silcretes (Nash et al., 1994), dolocretes, alcretes, or crusts made of manganese, titanium, gypsite (Taylor and Eggleton, 2001). It describes an indurated elemental layer usually found capping hills or surfaces, that appears to protect them from erosion (Taylor and Eggleton, 2001). They can be found all over the world, under different climatic conditions going from hyper-arid to tropical settings. In most cases, however, an environment with contrasting dry/wet seasons is needed (Campy and Macaire, 2003; Taylor and Eggleton, 2001; Nash et al., 1994; Tardy, 1981).

Duricrust formation is likely to depend on water availability, often linked to climatic conditions and, for certain types of duricrusts, on the minerals present in the regolith and/or the underlying protolith. To cite some examples, gypsite crusts form in hyper-arid areas (Watson, 1988), silcretes and calcretes form in arid environments (Nash et al., 1994), whereas iron duricrusts form in areas where more water is available during a certain period of the year (Tardy, 1993), and bauxitisation happens under tropical conditions (Retallack, 2001). Although no direct measurement of their rate of formation is yet available, one can estimate that the time needed to create a duricrust is of the order of 10^5 or more years (Tardy, 1993; Taylor and Eggleton, 2001).

Some formation hypotheses are considered similar for instance for ferricretes, silcretes or calcretes, but involving different elements (Campy and Macaire, 2003). For example, Nash et al. (1994)'s model of duricrust formation in the Kalahari Desert is mostly based on the characteristics of silica or carbonate duricrusts, not ferruginous ones, but his hypothesis of duricrust creation is still adaptable to almost every type of duricrust.

We will concentrate our study on ferricretes, also called ferruginous duricrusts, iron duricrusts or iron crusts, iron enriched levels or cangas (Tardy, 1993; Tardy and Roquin, 1998; Nahon, 1991; Paton and Williams, 1972; Ollier and Galloway, 1990; Vasconcelos et al., 1992; Monteiro et al., 2014; Vasconcelos and Carmo, 2018). Ferricretes are indurated layers made mostly of iron, with possible traces of other elements, e.g., titanium or manganese. Iron duricrusts form in a wide range of environments, as long as decisive wet and dry periods are observed: from tropical, subtropical to semi-arid up to arid environments. They can be found in Africa (Tardy, 1993; Tardy and Roquin, 1998; Tardy et al., 1991), South America (Girard et al., 2002; Tardy et al., 1991), India (Widdowson, 2009; Ollier and Sheth, 2008), and some paleocrusts can be found in Europe (Borger, 2000; Théveniaut et al., 2007; Strasser et al., 2009). Tardy (1993) provides specific conditions needed for the formation of duricrusts and defines a 'typical duricrust profile'. He describes iron duricrusts as "mostly monogenic, at least millions if not tens of

https://doi.org/10.5194/egusphere-2024-160
Preprint. Discussion started: 6 February 2024

millions of years old." They form in tropical climate with strong seasonality, which drives precipitation and dissolution cycles (Tardy et al., 1988). A climate conducive to the formation of iron duricrusts encompasses the following characteristics (Tardy et al., 1991; Tardy, 1993): 1) a mean annual rainfall, P, of around 1450 $m.yr^{-1}$, 2) a mean annual temperature, T, of ~28°C, 3) a mean relative air humidity of around 70~%, and 4) a long dry period of at least 6 months.

The preservation of iron rich levels and duricrusts through time depends on climate too. In semi-arid to arid areas, they are preserved and protect the regolith for longer periods of time than in subtropical to tropical areas as described by Taylor and Eggleton (2001); Tardy (1993). In these environments, erosion breaks down ferruginous duricrusts mostly physically, and iron blocks fall on lower parts of the topography and can, if they are not transported further, recompose themselves into new iron duricrusts or be incorporated into other formations (Taylor and Eggleton, 2001). In most cases today, ferricretes are observed capping and protecting hills, at the top of landscapes (Taylor and Eggleton, 2001).

There are currently two hypotheses for the formation of iron duricrusts: a hydrologically-based process (Taylor and Eggleton, 2001; Achyuthan, 2004; Widdowson, 2009; Bonsor et al., 2014; Riffel et al., 2016; Bourman et al., 2020) and a laterisation-based process (Tardy, 1986; Tardy et al., 1988; Nash et al., 1994; Tardy, 1993; Théveniaut and Freyssinet, 1999; Taylor and Eggleton, 2001), which are also referred to as horizontal and vertical models.

Hydrological hypothesis or horizontal model:

In this model, iron duricrusts form under a contrasting yearly climate, made of primarily wet and dry periods. During wet periods, the water table height is high and minerals, such as Fe_2^+, are transported from adjacent regions and accumulate. During dry periods, the water table height drops and minerals, such as Fe_3^+, precipitate. This cycle repeats itself for thousands of years, with the accumulation of iron elements leading to the formation of nodules, which, ultimately, cement into a ferruginous crust. In this case, no genetic link between the bedrock and the regolith beneath is needed nor described (Ollier and Galloway, 1990; Taylor and Eggleton, 2001). All elements are brought from adjacent sources through lateral transport. Also, duricrusts form at the water table, which means at multiple metres below the surface. It is generally accepted that, to permit accumulation of materials, the region needs to be tectonically inactive and that later periods of uplift (or base-level drop) are likely to exhume the duricrust to the surface where it becomes more resistant to erosion than the surrounding weathered material. Because they form at the water table level, i.e., close to valley bottoms and are often observed capping hilltops once they are uplifted and exhumed, exposed ferruginous duricrust are often considered to lead to 'landscape inversion' (Nash et al., 1994; Taylor and Eggleton, 2001) where former channels control the geometry of elongated hill tops.

Laterisation hypothesis or vertical model:

In this case, duricrusts are considered the ultimate stage of laterisation. Laterites are a type of tropical soil, encompassing "residual materials formed directly by in situ rock breakdown" (Widdowson, 2009). Laterites evolve through leaching and vertical transport of material. Easily soluble elements like sulfates, for example, are leached out of the regolith column, whereas insoluble elements or difficultly soluble elements like iron or manganese remain. All rock types can weather into laterites under the right conditions. However, only iron-rich or iron-bearing rocks evolve into ferricretes. Above the bedrock, the depleted

https://doi.org/10.5194/egusphere-2024-160
Preprint. Discussion started: 6 February 2024

saprolite, which can be tens of metres thick, is the thickest part of the profile. Above the saprolite, the mottled zone, is characterized by the accumulation of iron nodules and bleached spots, giving it a mottled appearance. With time, the open pores left through leaching close by compaction and cementation of iron nodules, leading ultimately to the formation of a ferricrete (e.g., Tardy and Roquin (1992); Taylor and Eggleton (2001); Tardy and Roquin (1998); Nahon and Bocquier (1983); Nahon (1991)). In this case, a clear genetic link can be observed between the bedrock, the overlying regolith and the ferruginous duricrust, which is likely to be reflected in their geochemical signature (Tardy, 1993). Also, to have enough material transported vertically, a constant, but slow uplift (or base-level drop) is needed to provide enough material (iron) to form the duricrust. A contrasting climate appears also to be an important condition for the formation of duricrusts through laterisation (Tardy, 1993; Taylor and Eggleton, 2001). Lateritic duricrust formation happens near the surface, or even at the surface, contrary to the hydrological formation hypothesis.

It is worth noting that duricrusts can also form through the erosion and breaking off of duricrusts that formed at high elevations. The resulting debris accumulate and cement at lower topographies to form "reconstructed" duricrusts. In this case, duricrusts can be genetically linked to multiple other duricrusts (through dating of the nodules), as they can form by mixing (Taylor and Eggleton, 2001).

There exists, at this stage, no numerical model for the formation of duricrusts, apart from the conceptual model developed by Nash et al. (1994) and the highly simplified model developed by Sacek et al. (2019) to estimate the effects of duricrust formation on erosional patterns at the continental scale. Our main objective is to present a simple, yet predictive numerical model to simulate the geometry and timing of duricrust formation on geological time scales, to predict their effect on surface processes and to compare them to observations. In other words, we propose here to develop a new parametric representation of the process of duricrust formation based on a reduced set of generic parameters that can be constrained by comparing the model predictions to observations, rather than using a representation that would required the calibration of parameters through direct experimentation or measurements.

We will focus here in developing a model for duricrust formation based on the hydrological hypothesis (or horizontal model). We are in the process of developing another model based on the laterisation hypothesis (or vertical model), which we plan on detailing and comparing to the model presented here in a future publication.

2 Method and Results

2.1 Existing regolith formation model (Braun et al., 2016)

Duricrust formation takes place within the regolith, i.e., a layer at the Earth's surface that is formed by the progressive weathering of the underlying basement. In the last decade, several models for regolith formation have been proposed including Lebedeva et al. (2007), Ferrier and Kirchner (2008), Brantley and White (2009), Maher (2010), Lebedeva et al. (2010), Pelletier (2010), Lebedeva and Brantley (2013), Norton et al. (2014), Pelletier et al. (2016), Braun et al. (2016), Brantley et al. (2017) or Lebedeva and Brantley (2018). They rely on a variety of approaches combining various physical, chemical, and hydrological processes.

https://doi.org/10.5194/egusphere-2024-160
Preprint. Discussion started: 6 February 2024

Here we will use the model for regolith formation developed by Braun et al. (2016) that computes the rate of downward migration of a weathering front in proportion to the velocity of the water in the overlying permeable regolith. This model is highly suited for our purpose as it predicts the evolution of the regolith layer and the geometry of the water table over geological time scales. It needs to be adapted for our purpose as it assumes that the regolith layer has uniform physical properties (hydraulic conductivity, resistance to erosion, etc.) and cannot predict the seasonal cycles of the water table. The model was designed to work at the scale of a 'hill' (i.e., from tens of metres to tens of kilometres) connected to an arbitrary base level (a river, a lake or an ocean) (see figure 1).

Braun et al. (2016)'s model is made of three components: a surface process model, a hydrological model and a weathering model. The surface process model assumes that the evolution of surface topography is controlled by tectonic uplift U and transport of sediment assumed to be proportional to local slope, leading to the following diffusion equation:

$$\frac{\partial z}{\partial t} = U + \frac{\partial}{\partial x} K_D \frac{\partial z}{\partial x} \tag{1}$$

where U is uplift rate (or base-level drop rate), z the topographic height, K_D a surface transport coefficient (or diffusivity), and x and t the spatial and temporal coordinates. Topography is assumed to be fixed at base level on one side of the model ($x = 0$) while the other side (at $x = L$) corresponds to the top of the hill where surface topography gradient is assumed to be nil. The hydrological model is based on the Dupuit-Forchheimer assumptions that flow is dominantly lateral and that discharge is proportional to the saturated aquifer thickness, leading to the following continuity equation governing the height of the water table, H:

$$K(H - z + B)\frac{\partial H}{\partial x} + \int_L^x P \, dx' = 0 \tag{2}$$

where B is the thickness of the regolith layer, K its hydraulic conductivity and P is precipitation rate. The water table is assumed to be fixed with respect to the topography at $x = 0$. Finally, the weathering model assumes that the weathering front propagates at a velocity that is proportional to the velocity of the fluid, product of the water table gradient by the hydraulic conductivity, according to:

$$\frac{\partial B}{\partial t} = FK\frac{\partial H}{\partial x} - \frac{\partial z}{\partial t} \tag{3}$$

where F is a dimensionless parameter that represents the ratio between the weathering front advance velocity and the fluid velocity and is therefore very small ($\approx 10^{-6} - 10^{-8}$).

https://doi.org/10.5194/egusphere-2024-160
Preprint. Discussion started: 6 February 2024

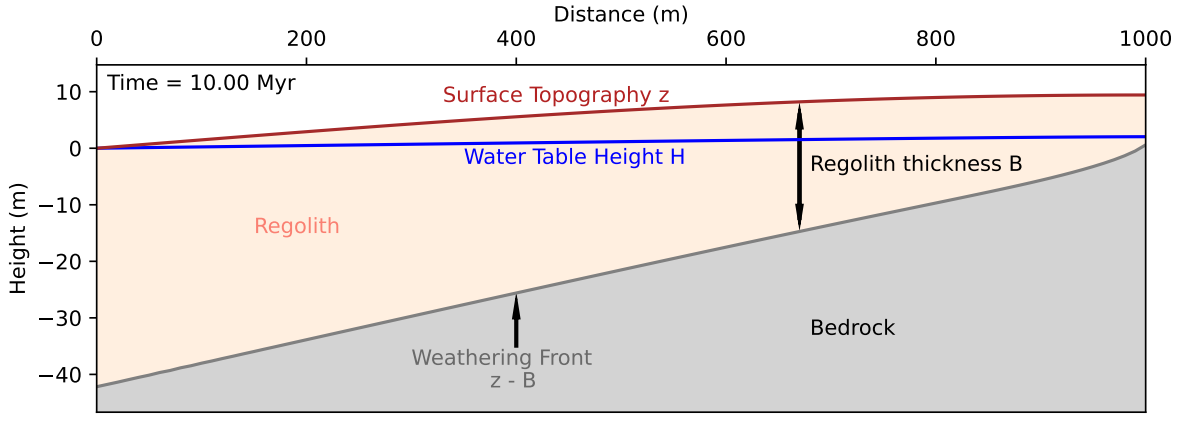

Figure 1. Problem geometry with quantities and variables as defined in Braun et al. (2016) and displayed on a steady-state configuration obtained by solving the set of differential equations given in the text for the weathering front velocity (weathering front in dark grey), the geometry of the water table (water table in blue) and the rate of surface erosion (topography is brick red). Result after 10 Myr.

We implemented Braun et al. (2016)'s model into the Xarray-simlab framework (Bovy et al., 2021). The hill topography, water table and regolith thickness shown in figure 1 are the result of a 'basic' model run on a 1000 m long and initially 20 m high hill, with the water table shown in blue, the surface topography in brown and the weathering front in grey, separating the regolith layer (beige) from the underlying bedrock (dark grey). We see that, for the model parameters used, i.e., $K_D = 1$, $U = 10^{-5}\ m.yr^{-1}$, $K = 10^{4}\ m.yr^{-1}$, $P = 1\ m.yr^{-1}$ and $F = 10^{-6}$, the system reaches a steady-state geometry, with regolith thickness increasing from the top to the bottom of the hill.

Braun et al. (2016) showed that the predicted steady-state regolith geometry depends on the value of two dimensionless parameters, Ω and Γ, defined as:

$$\Omega = \frac{FKL}{2K_D} = \frac{FK\bar{S}}{U} \quad \text{and} \quad \Gamma = \frac{K\bar{S}^2}{P} \tag{4}$$

where $\bar{S}$ is the mean surface slope. On the one hand, Ω controls the thickness of the regolith layer, i.e., Ω must be greater than unity for any regolith to develop at the top of the hill and Ω must be greater than 0.5 for regolith to develop everywhere along the hill. On the other hand, Γ controls whether the regolith is thickest at the top of the hill, i.e., when $\Gamma > \frac{\Omega^2}{\Omega-1}$, or thickest at the base of the hill, i.e., when $\Gamma < \frac{\Omega^2}{\Omega-1}$. For the model results shown in figure 1, the values of Ω and Γ are 5 and 0.25, respectively, which explains why the regolith is thickest at the base of the hill, as $\Gamma < \frac{\Omega^2}{\Omega-1} \approx 6$.

2.2 New duricrust model

To model the formation of ferricretes, we added the dimensionless quantity κ, or erodability parameter, that represents the relative strength, or more exactly the relative resistance to surface erosion of the material within the regolith layer. The parameter κ is allowed to vary between 0 and 1, both horizontally and vertically, i.e., $\kappa = \kappa(x, y)$, where y is a distance measured from

https://doi.org/10.5194/egusphere-2024-160
Preprint. Discussion started: 6 February 2024

the base of the regolith layer. To constrain the time evolution of κ, we use an additional, fourth equation that represents the hardening process within the beating range of the water table:

$$\frac{\partial \kappa}{\partial t} = -\frac{\kappa}{\tau}\frac{P}{P_{ref}}\mathrm{e}^{-(y-y_w)^2/\lambda^2} - v_W\frac{\partial \kappa}{\partial y} \tag{5}$$

where y_w is the height of the water table depth measured from the base of the regolith, λ is the assumed water table beating range (in m), τ is the assumed characteristic time for regolith hardening (in years), P_{ref} represents a reference precipitation rate (in $m.yr^{-1}$), v_W is the weathering front vertical propagation velocity given by:

$$v_W = FK\frac{\partial H}{\partial x} \tag{6}$$

as described in Braun et al. (2016), equation 5 contains two parts. The first one represents the self limiting process of hardening that is only taking place in the vicinity of the water table, i.e., within a distance equal to the water table beating range, λ, and is assumed to be proportional to precipitation rate, the prime controlling factor on flow velocity and thus on the transport and precipitation of iron. The second one represents the advection of the regolith (and thus of the hardening parameter) with respect to the weathering front.

As portrayed in figure 2, the variable κ is also used in an updated version of the erosion equation (1), to account for the increased surface resistance to erosion due to the formation of a duricrust, according to:

$$\frac{\partial z}{\partial t} = U + K_{D,0}\frac{\partial}{\partial x}\kappa(x, y=0)\frac{\partial z}{\partial x} \tag{7}$$

where $K_{D,0}$ is a reference transport coefficient or diffusivity, i.e., corresponding to a regolith that has not been subjected to any hardening. Note also that equation (5) predicts a range of κ values starting from unity for a fresh regolith, i.e., that has not been subjected to any hardening, to infinitely small values. In order to define when a duricrust has effectively been formed, we arbitrarily select a threshold value of $\kappa = \kappa_D = 0.2$, which corresponds to the formation of a layer that is five times more resistant to erosion than the surrounding regolith. This arbitrary choice is made in order for the resulting surface topography to present a clear step where the duricrust has formed.

https://doi.org/10.5194/egusphere-2024-160
Preprint. Discussion started: 6 February 2024

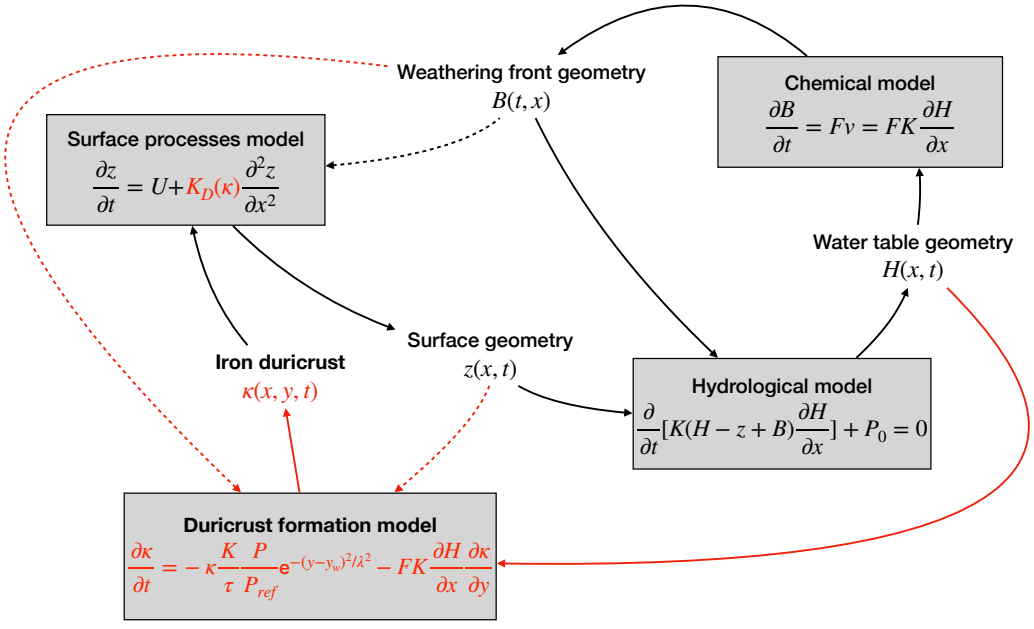

Figure 2. Connectivity between the four parameters in the new model, modified from Braun et al. (2016). We see the hydrological model, the surface process model and the chemical model (Braun et al., 2016). The new (highlighted in red) duricrust formation model is based on the hardening coefficient κ. It is directly connected to the hydrological model by the water table geometry H and the surface processes model by κ (concrete arrows), and indirectly influenced by the weathering front geometry B, and surface geometry z (dashed arrows).

To ensure accuracy and stability of the numerical solution to this equation, we employed the total variation diminishing method (Leer, 1974) combined with a simple 1D finite volume method along the y-direction (Campforts and Govers, 2015). In all numerical experiments shown here, the model resolution was set to 101 points in the horizontal x-direction and 501 points in the vertical y-direction. Time stepping was controlled by the Courant condition that imposes that material cannot be advected by more than one grid spacing per time step. Note that the model is not truly two-dimensional as the evolution of the surface topography, water table height and weathering front are computed in the x-direction only and κ is computed in the y-direction only; i.e., there are no partial differential equation in the model that depends on both spatial coordinates.

Finally, it is worth noting that, as seen in figure 2, the model is made of four different processes, each being represented by its own differential equation and linking four unknowns: z, the topographic elevation, B, the regolith thickness, H, the water table height and κ, the erodability parameter. As more than one unknown appear in each equation, these equations are coupled. However, in our solution scheme, we solve them sequentially.

This heuristic approach to the parametrisation of the process of regolith hardening or armouring is based on first-order field evidence. A more mechanistic approach would have required estimates of chemical and physical rate constants that are poorly defined (such as the solubility of iron in its various valence forms), especially under natural conditions. Furthermore, as noted

https://doi.org/10.5194/egusphere-2024-160
Preprint. Discussion started: 6 February 2024

by Beauvais (2009); Monteiro et al. (2014, 2018), for example, the formation of iron duricrusts (or cangas) is also strongly controlled by biological processes but a proper quantification and parametrisation of this effect is, so far, lacking and cannot be at this stage included in a long-term model for duricrust formation as presented here.

2.3 Constraining new model parameters

Compared to Braun et al. (2016)'s regolith model, our parametrisation introduces two new model parameters: τ and λ. Firstly, the characteristic time for regolith hardening (or duricrust formation), τ, can be constrained by various chronometric methods. Most studies have been carried out during the last century, by authors e.g. Leneuf (1959); Gac (1980); Boulangé (1984); Tardy and Roquin (1992); Boulangé et al. (1997); Paquet and Clauer (1997) who have tried to describe duricrust formation rates in the African, South-American and Australian regions. Note that in citing them, we have included estimates of laterisation rates and ages for duricrusts assumed to form through laterisation too, as too few data are available for ferricrete formation under the hydrological hypothesis alone, which would lead to a bias. As noted by Retallack (2010) iron duricrust dating did not take place until recently. The focus had been placed on dating laterites or bauxites (e.g. Tardy and Roquin (1992); Tardy (1993); Théveniaut and Freyssinet (1999); Ricordel-Prognon et al. (2010); Tardy and Roquin (1998); Guinoiseau et al. (2021)). New studies (Chivas and Atlhopheng, 2010; Allard et al., 2018; dos Santos Albuquerque et al., 2020; Heller et al., 2022) using new methods using oxygen isotopes or iron oxide dating with (U-Th)/He geochronology for example, have concentrated on kaolinites and ferricretes. Most rates derived from ages were indirectly calculated by using paleomagnetic and thermochronological methods (Vasconcelos and Carmo, 2018; Théveniaut and Freyssinet, 1999; Théveniaut et al., 2007) and regolith profile descriptions. In some cases, estimated erosion rates helped constrain presumed thickness, however in other cases, duricrust thicknesses were not available. Some studies also constrained laterite and duricrust ages only, without providing formation rates because of lack of data. These ages are however a way for us to constrain the upper boundary for τ. As can be seen, it is therefore a difficult task to gather precise duricrust formation rates. Here, we provide a range of estimates of minimum and maximum values for duricrust formation time spans and corresponding formation rates.

Tardy (1969) estimated through geochemical calculations the time necessary to transform 1 m of pure granite into kaolinite in temperate climates at approximately 100 000 yrs. According to Tardy and Roquin (1992), "1000 mm of water percolating each year through a profile allows the formation of 1 m of kaolinite lithomarge and consequently allows a lowering of the weathering fronts of 10 m per Myr or 1000 m per 100 Myr". Benedetti et al. (1992) describe basalts in Brazil "continuously evolving" since 700 000 yrs ago. These ages were computed using geochemical properties of percolating waters and their associated weathering products.

Théveniaut and Freyssinet (1999) did a paleomagnetic study on lateritic profiles in French Guinea. A duricrust cap of 14 metres was analysed and determined to have formed during two laterisation events, an older one, with a minimum age of 10 Ma, and a younger one, with a contemporary age. We approximated a duricrust formation rate of around 1.5 m.Myr^{-1}. Saprolitisation rates were however calculated more precisely by Théveniaut and Freyssinet (1999), giving a $11.3 \pm 0.5\ m.Myr^{-1}$. Later, Théveniaut et al. (2007) describe a profile called "la borne de fer" in the North-Eastern part of France, where a multiple-metre thick iron duricrust is found just below the surface of a 450 m high hill dated by paleomagntic means to be of at least

https://doi.org/10.5194/egusphere-2024-160
Preprint. Discussion started: 6 February 2024

Barremian age (Théveniaut et al., 2007). This suggests a minimum formation rate of ~1 $m.Myr^{-1}$. In Chad, Tardy and Roquin (1992) suggest a landscape lowering rate by chemical erosion to produce ferricretes of 0.1 km in 1 Byrs (0.1 km/1000 Myrs). In Malagasy, laterisation rates range up to 3.3 km/Byr (3.3 km/10^9 yrs) (Tardy and Roquin, 1992). It would take longer to form lateritic profiles to the last beauxite/ferricrete stage (30 Myrs for 75 m).

Vasconcelos and Conroy (2003) performed $^{40}Ar/^{39}Ar$ laser incremental heating analyses on samples from weathering profiles from 11 sites in the Dugald River area (Queensland, Australia), across 3 distinct elevations. They observed that the higher the samples is collected from, the older the age is, ranging from 16 to 12 Ma at high elevation, 6 to 4 Ma at mid-elevation and 2.2 to 0.8 Ma near the base of the section. With these ages, they estimated a weathering rate in the regolith of 3.8 $m.Myr^{-1}$ in the region over the last 15 Ma. In western Africa, Beauvais (2009) dated weathering profiles using $^{40}Ar/^{39}Ar$, and found ages in episodic phases. At the top of the profile, ages range from 59 - 45 Ma in the ferro-manganese crust and deeper below, ages from 3.4 - 2.9 Ma were registered at the weathering front. However, evidence for episodic weathering from two other periods in the Miocene, namely 29 to 24 Ma and 18 to 11.5 Ma were registered. Those periods were usually divided by erosional periods. Hénocque et al. (1998) studied the site of Tambao in Burkina Faso, where lateritic ore deposit manifest and are mined. Rate of cryptomelane precipitation were determined through $^{40}Ar/^{39}Ar$, ranging from 1 to 5 $mm.Myr^{-1}$. In Brazil, studies around the Quadrilaterro Ferrifero (QF), Vasconcelos and Carmo (2018) report regolith ages of up to 70 Ma old. On the top of Cordilleras in that region, thick cangas cover the topography with thicknesses up to 50 m. Taking into account their estimated erosion rates, a minimum formation rate of cangas in the QF would be approximately 0.03 $mm.Myr^{-1}$, while ignoring erosion and taking into account climatic changes, a maximum rate could be more than 1 $m.Myr^{-1}$.

Leneuf (1959) determined a rate of ~5 $m.Myr^{-1}$ for kaolinite formation at Lakota and Boulangé (1984) observes 1.4 $m.Myr^{-1}$ on Mount Tato (Ivory Coast). Paquet and Clauer (1997) describe two profiles in the same area as Leneuf (1959), in the Ivory Coast. They conclude that 15 m of bauxite require 45 m of granite in the first case. In the second case, Paquet and Clauer (1997) describe a rate of beauxitisation of 3 $m.Myr^{-1}$ with data from Fritz and Tardy (1973). Boulangé et al. (1997) report landscape lowering rates from bauxite formation on granite in the Ivory Coast of 30 m to form 15 m of bauxite and up to a 70~% volume reduction to form the pisolitic bauxite overlying the main bauxite. They report this taking from 3 to 5 Myrs. Gac (1980) determines a beauxitisation rate of 1.35 $m.Myr^{-1}$ in the Chad Chari basin (Chad). One of the first studies about duricrust ages is by Boulangé et al. (1997) quote a 90 m lowering of Cretaceous sandstones and mudrocks in Brazil to form 10 m of sandy residuum over bauxite; this would, according to their calculations, take between 30 and 100 Myrs to achieve. In similar environments, Horbe and Anand (2011) propose that bauxite take between 15 to 20 Myrs to form.

In more recent years, new techniques have been developed to try and date iron duricrusts by thermochronology (Wells et al., 2019). Using those, authors such as dos Santos Albuquerque et al. (2020) estimate formation times ranging from 10 to 15 Myrs for metre-thick iron and bauxitic duricrusts. Heller et al. (2022) have dated iron nodules from bauxitic duricrusts in North-western Brazil. Ages span from 30 Ma to today. The ages seem to belong to three distinct formation episodes spanning from 4 Myrs to 1 Myr. Considering the mean duricrust thickness of 5.5 m in the area, these ages yield a formation rate estimate ranging between 1.4 and 5.5 $m.Myr^{-1}$.

https://doi.org/10.5194/egusphere-2024-160
Preprint. Discussion started: 6 February 2024

Some authors describe ages without weathering rates. The lack or complexity of data make it difficult to evaluate weathering rates, however, they give valuable information for constraining the upper values for τ. Ricordel-Prognon et al. (2010) date iron oxides in ferruginous clays of a profile in the French Massif Central with paleomagntic methods. The lateritic profile is not complete, as no cap is observed. First believed to be Lower Tertiary, it is proved by Ricordel-Prognon et al. (2010) the clays to be Late Jurassic to early Cretaceous. In French Guiana, Théveniaut and Freyssinet (2002) record beauxitic and ferruginous duricrust ages at 3 different periods, defined by the described units observed. For the first, highest unit, the recorded ages are 60, 50 and 40 Ma; while for the second and third units, Miocene ages are registered, with 13 and 10 Ma for the second unit and ages spanning across the Late Miocene for the third unit. Cryptomelane dating was done in Western Africa by Chardon (2023), with interpreted bauxitisation periods mostly between 59 and 45 Ma, with main cluster from 50 to 45 Ma. Duricrusting of ferricretes also happened between 29 and 24 Ma. Weathering took place between 40 and 29 Ma, accordingly, the bauxite weathering period has started during the Early Paleocene. Another phase of bauxitisation is dated to be Late Miocene, around 14 to 6 Ma for the Cameroon Rise. These ages accumulated from previous literature are used here to determine paleosurfaces and their evolution.

https://doi.org/10.5194/egusphere-2024-160
Preprint. Discussion started: 6 February 2024

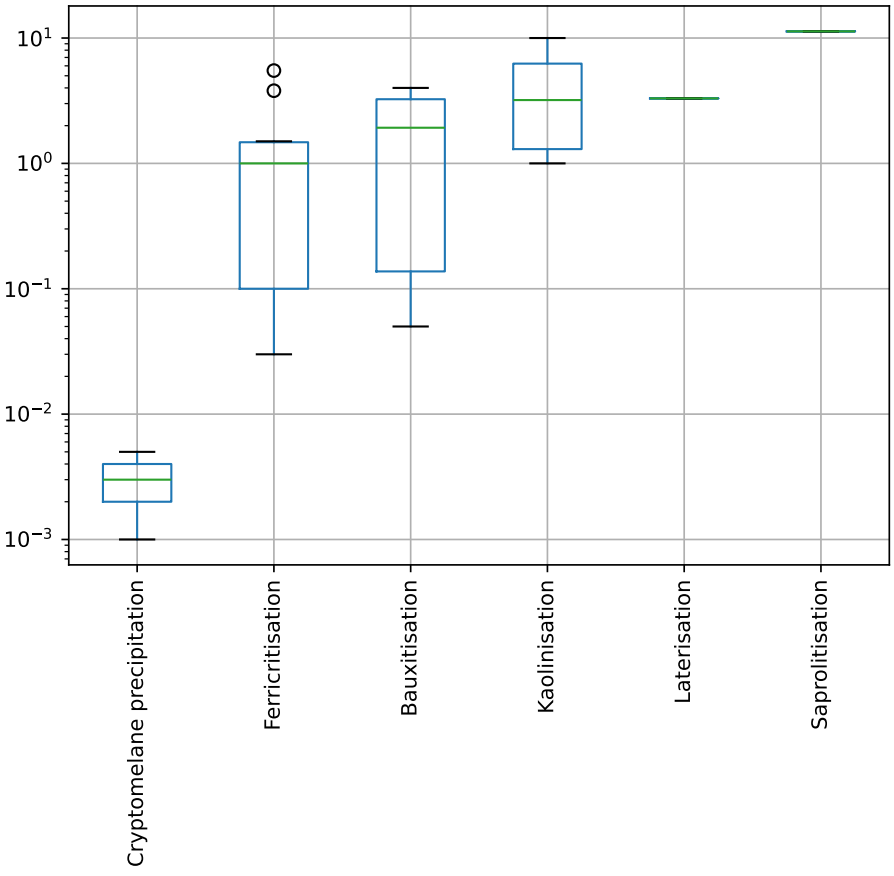

Figure 3. In this statistical box-plot representation, the green line represents the mean value, the blue box encompasses values from the lower quartile to the upper quartile, while the black whiskers limit at 1.5 of the interquartile range. The black circles represent outliers. Six different categories of weathering processes can be differentiated on the x-axis with their respective rates on the log y-axis as derived from literature. The summarized rates include given rates by authors, but also our estimates inferred from the cited literature. For a figure without our estimates, and rates only from literature, figure A1 in the appendix is available.

The rates are summarized in figure 3 as a function of the dominant process. We see that the time span necessary for the formation of an approximately one metre thick duricrust is of the order of a few tens of thousands to millions of years. At this stage it is therefore not feasible to better constrain the value of the parameter τ. In a way, this also confirms that developing a more sophisticated model, i.e., requiring more rate-dependent parameters, is not justified. It also highlights the need to obtain more accurate and/or more abundant age constraints pertaining to the formation rates of ferricretes.

The second model parameter, λ, is the water table beating range (or water table fluctuation, WTF). It can be constrained by direct observations of the change in water table height over the seasonal cycle, which ranges from a few centimetres to multiple metres, depending mostly on the seasonal variability of rainfall (Tardy, 1993; Taylor and Eggleton, 2001). Water

https://doi.org/10.5194/egusphere-2024-160
Preprint. Discussion started: 6 February 2024

table seasonal fluctuations have been monitored for e.g. agriculture (Chandra et al., 2015), health, pollution (Deng et al., 2014) or water availability (Balugani et al., 2017). Groundwater studies have registered water table heights all across the globe. Here, we used studies from different climatic regions to calibrate the water table beating range in our model, including, for completeness, environments where duricrusts are known to form and others. Leduc et al. (1997) describe seasonal water table fluctuation in southern Niger in the Sahel aquifer, known for its tropical semi-arid climate, with a long dry season and short wet season. The registered fluctuation in the 223 analysed wells ranges from 0 to 9 metres. Temgoua et al. (2005) describe WTF of about 2 metres in the humid tropical zone of southern Cameroon, where massive ferruginous duricrusts form on footslopes of hills. Hassan et al. (2014) worked in the Sardón Catchment near Castilla y León, Spain. The climate is Mediterranean semi-arid, and most rain events take place during Spring. The yearly WTF is ~2 metres (Hassan et al., 2014). Hassan et al. (2014) cites a study from Ely and Kahle (2012), in Washington State (USA), where they analysed hydrological data from the Chamokane Creek basin. Hydrographs from the area showed WTF in the range 2 to 9,9 metres, with a mean value around 5.5 metres. In South-Korea, Moon et al. (2004) analysed monitoring data from 66 wells across the whole country, where the climate is temperate. Results show maximum variability in water-table fluctuation of 0.94 to 3.68 metres. Multiple studies in India registered water table fluctuations across semi-arid tropical (Sreedevi et al., 2006; Kuruppath et al., 2018; Bhuiyan, 2010) environments controlled by monsoons (Chandra et al., 2015; Kuruppath et al., 2018). Sreedevi et al. (2006) analysed aquifers in Archean granites in the Maheshwaram watershed. Seasonal water table fluctuation was registered to be 4.2 to 5 metres between May and December (pre- and post-monsoon). Maréchal et al. (2006) have analysed wells in the same region, with WTF of 2 to 6 metres. In the Rajasthan state, in the Aravalli range, Bhuiyan (2010) observed a mean WTF in multiple geomorphic classes. He also measured WTF under pediments (mean WTF 3.61 m) and buried pediments (mean WTF 3.09 m). Mean WTF in this study is 3.35 metres. In another part of India, on the eastern part of the Chotanagpur plateau, bedrock of Archean to Paleozoic ages formed pediplains (Chandra et al., 2015). WTF ranges there from ~0.2 to 5 metres. Similar values were registered in the Karur district, with pre- and post-monsoon water table heights varying between 0.2 and 6.6 metres (Chandra et al., 2015). Average WTF for the North-eastern monsoon is 2.5 metres and 1.6 metres for the South-western monsoon (Kuruppath et al., 2018). Bhuiyan (2010); Chandra et al. (2015) registered WTF under pediments and what could be indentified as ferricretes, with mean water table fluctuation being 3.41 m and 1.77 m respectively. In Southern China, Deng et al. (2014) analysed groundwater monitoring data from 39 wells in the Jianghan alluvial plain. The study focused on arsenic concentration in the water and water table fluctuation patterns. The climate in that region is sub-tropical, and controlled by monsoons. Registered WTF is about 1 to 2 metres. In Minas Gerais, Brazil, where active duricrusting and weathering is taking place today, Marques et al. (2020) registered WTF from 2011 to 2018. A very low seasonal fluctuation is registered, with values around 1 metre. In temperate to cold humid climate zones, groundwater recharge is highly dependable on snow cover and seasons (Nygren et al., 2020). In Finland and Sweden, Nygren et al. (2020) have analysed data from a 31 year-long monitoring dataset from 264 piezometers. Seasonal WTFs are the lowest for the region, with values under 1 metre.

Constraining λ can thus be done according to climatic regions. In semi-arid environments, the beating range is of the order of several metres, with maximum values of ~10 metres. In tropical, monsoon driven climates, WTF is around 2 to 3 metres,

https://doi.org/10.5194/egusphere-2024-160
Preprint. Discussion started: 6 February 2024

sometimes less. In temperate and cold climates, water table seasonal fluctuations are of the order of a metre. A summary of those values is given in figure 4.

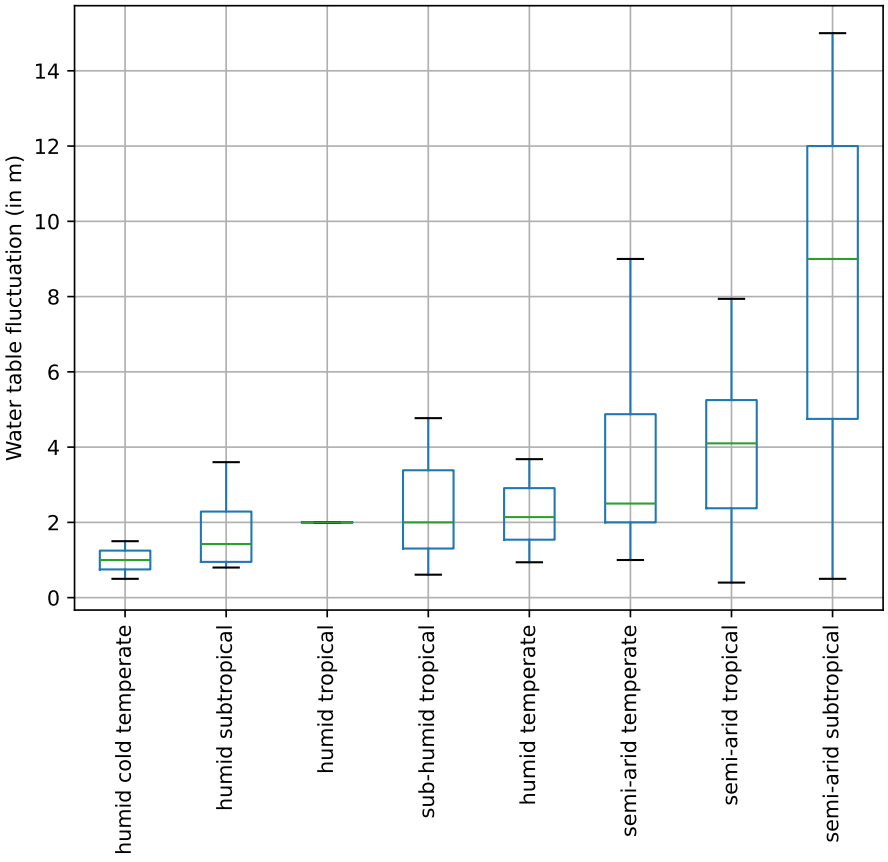

Figure 4. Summary in boxplot representation of literature review about yearly water table fluctuations in modern systems. Data are divided in seven different environments on the x-axis, classified by climatic conditions. In this statistical box-plot representation, the green line represents the mean value, the blue box encompasses values from the lower quartile to the upper quartile, while the black whiskers end at the lowest and highest values of the dataset.

2.4 A simple model run

To illustrate the behaviour of the new model, we performed an experiment on a hill of length 1000 m. The parameter values are identical to those used in the experiment shown in figure 1, except for the uplift, which is here a cyclic function alternating periods of uniform uplift (or base-level drop) at a rate $U_0 = 50^{-6}\ m.yr^{-1}$ with periods of tectonic quiescence ($U = 0$). Each period is of duration $\Phi = 500$ kyr long and the model runs for $t_f = 10$ Myrs. P is constant and equal to the reference precipitation $P_{ref} = 1\ m.yr^{-1}$. The other two parameters introduced by the duricrust formation model are set at $\lambda = 3$ m and $\tau = 50$ kyrs.

https://doi.org/10.5194/egusphere-2024-160
Preprint. Discussion started: 6 February 2024

In figure 5 we show the resulting hill, regolith and duricrust geometries at the last time step. We see that at the level of the water table (in blue), a duricrust has formed. The colour gradient used in the regolith layer represents the values of κ, the erodability, varying between 1 (beige) and tending to 0 (dark red). When κ values are close to 1, the regolith is unaltered. Below the threshold of $\kappa < \kappa_D$, we consider that a hardened duricrust has formed. We also see that below the water table, the regolith, in beige, is unaltered. However, above the water table, the regolith tends to show signs of hardening, with κ values comprised between 0.9 and 0.5. The duricrust layer itself ($\kappa < \kappa_D$) forms around the water table, and has a thickness of approximately 4 m (similar to the assumed value for λ). This behaviour results from the vertical advection of material during periods of tectonic activity in response to uplift (or base-level drop) and surface erosion. Rocks from the intact bedrock are subjected to intense weathering as they traverse the weathering front at the base of the regolith layer. They are then exhumed towards the surface until they are eroded away. In doing so, they cross the water table and its beating range where they are subjected to hardening by iron transport and precipitation to form a duricrust if the time spent near the water table is longer than the assumed time for hardening, τ. This, they do only during the period of tectonic quiescence. The partial hardening that is observed in the regolith above the duricrust corresponds to a period of active tectonics and uplift (or base-level drop) during which rocks within the regolith traverse the water table but do not stay in its vicinity long enough for the hardening process to lead to the formation of a duricrust (κ remains smaller than κ_D).

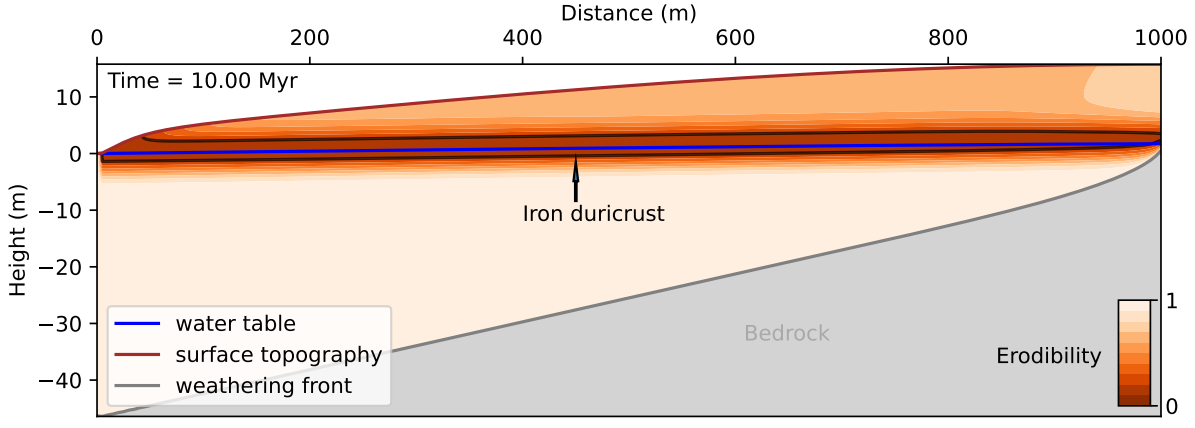

Figure 5. Problem geometry with quantities and variables as defined in the new model and Braun et al. (2016), with added iron duricrust formation, displayed on a steady-state configuration, on a 1000 m long distance. The erodability coefficient κ concerns the regolith. The lighter the colour, the softer/more erodible is the material, and the darker the colour, the harder/less erodible the material. The ferricrete, in dark red, is highlighted with an outline in black lines, corresponding to the threshold κ_D. The result shown is at the last time step, which corresponds to 10 Myrs.

Comparing the results of the model with figure 5 and without (figure 1) duricrust formation, we see that the solutions at the last time step are similar: the regolith has the same thickness and geometry (thicker near the base of the hill) and the surface topography geometry is similar too. However, this similarity disappears when looking at intermediary times steps, as shown

https://doi.org/10.5194/egusphere-2024-160
Preprint. Discussion started: 6 February 2024

in figure 6 and in the animation A2 in the supplementary material. In figure 6, we illustrate one complete cycle of duration $2 \times \Phi$, which includes one uplifting and one quiescent period of time (duration of a cycle). It thus covers a time span of 1 Myr, from 3.80 Myr to 4.80 Myr in the model evolution (figures 6a) and i)). The first period (figure 6a), b), c) and d)) is marked by no tectonic activity. From figure 6a) to c), we can observe the formation of an indurated layer at the water table level. We see that during the periods of active uplift or base-level drop (figure 6d), e), f) and g)), the duricrust that has formed in the vicinity of the water table is progressively exhumed as it is subjected to surface erosion. Being characterised by values of κ that are smaller than κ_D, the hardened layer (duricrust) is less erodible and causes the formation of a topographic step along the hill surface. This step also causes the surface slope beneath the duricrust to steepen, which leads, in turn, to an increase in the hill mean and maximum topography. During the following period of quiescence (figure 6h) and i)), the exhumed duricrust temporarily protects the top of the hill from erosion (figure 6h)) until it is removed (figure 6i)), initiating a phase of rapid surface topography lowering. During this quiescence phase (figure 6i)), we also note a new duricrust forming at the water table level.

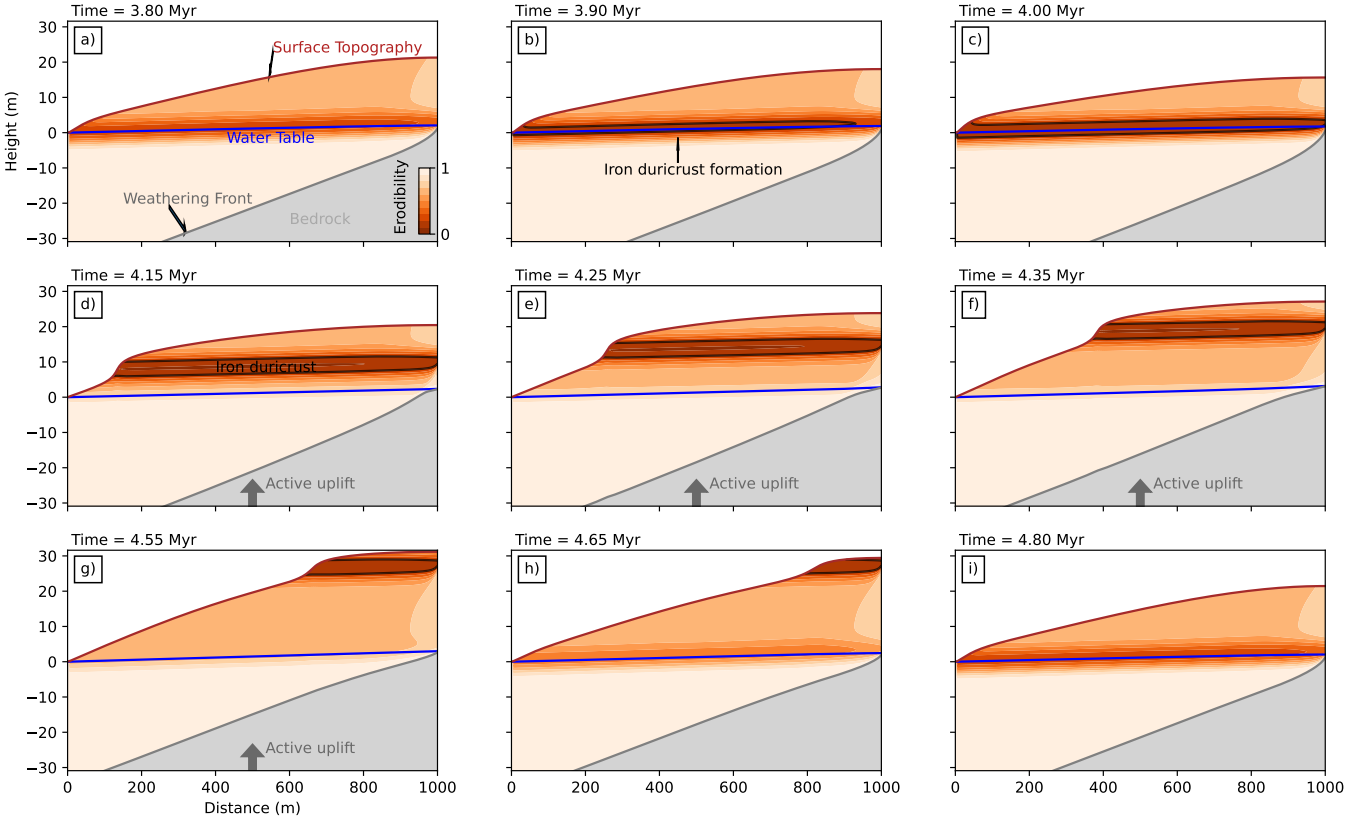

Figure 6. From a) to i): Problem geometry across time. The chosen time frame is from 4.15 Myrs (a) to 4.80 Myrs (i). The chosen time frame corresponds to one cycle, Φ. Evolution of duricrust formation (a) from the water table to exhumation (i). Sections a) to c) and g) to i) are without uplift (or base level drop), while section d) to f) have active uplift, highlighted by a grey arrow.

https://doi.org/10.5194/egusphere-2024-160
Preprint. Discussion started: 6 February 2024

This evolution of the topography is summarized in figure 7 where we compare the time evolution of the maximum topography (i.e., at the top of the hill) predicted in the reference model run shown in figure 5 with the prediction of an almost identical model experiment in which we prevented the formation of duricrust by setting τ to a very large value. We see that the experiment that includes the duricrust is characterised by higher topography but, interestingly, both experiments show a rapid decrease in maximum topography immediately following the end of the period of tectonic activity. There is no delay in the decay (or preservation) of the topography caused by the presence of the duricrust.

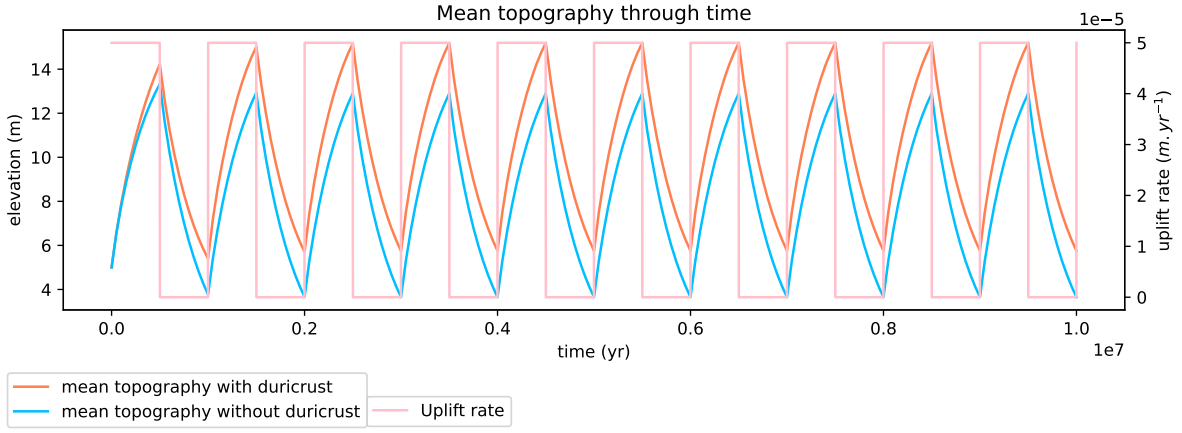

Figure 7. Mean topography elevation for two model experiments responding, through time, to the same periodical uplift rate. In orange: mean topography elevation through time with ferricrete formation. In blue: mean topography elevation through time without ferricrete formation.

The geometries that can be created by the model are varied and we cannot reproduce them exhaustively here. One case that is very relevant to many natural systems involves the presence (or preservation) of a family of duricrusts in the same landscape. Although this is likely to take place on a much greater scale than that of a single hill, we show in figure 8a) results of a model run in which three generations of duricrust have been preserved at the end of a period of quiescence. This has been achieved by lowering the value of the characteristic time τ leading to more rapid and therefore more intense lowering of the value of κ in the vicinity of the water table. The resulting duricrusts have become stronger and have been preserved during two cycles of uplift/quiescence and erosion.

In figure 8b) we show the computed ages of the duricrust and the regolith. In the hardened layers (i.e., where $\kappa < \kappa_D$) the ages correspond to the time where the hardening took place. In the unaltered or partially altered regolith (i.e., where $\kappa > \kappa_D$) ages correspond to the time where the rocks crossed the weathering front at the boundary between the regolith layer and the underlying bedrock. In figure 8b), we see that the youngest duricrust is still forming at the water table level, while the oldest duricrust is now at the top of the hill and is almost 2 Myrs old. The middle duricrust has an age that is the mean of the other two. While the evolution of duricrusts in the regolith enables aging of uplifting duricrusts, regolith layers also age. Regolith ages depend on the position of the weathering front. Thus, the youngest regolith is at the base of the weathering profile, while the

https://doi.org/10.5194/egusphere-2024-160
Preprint. Discussion started: 6 February 2024

oldest regolith is outcropping at the top of the hill. Duricrust and regolith ages do not correspond, having inter-located layers of older regolith in-between two duricrusts. However, it is interesting to note that the difference between regolith and duricrust ages is greatest near the base level and decreases beneath the hill top.

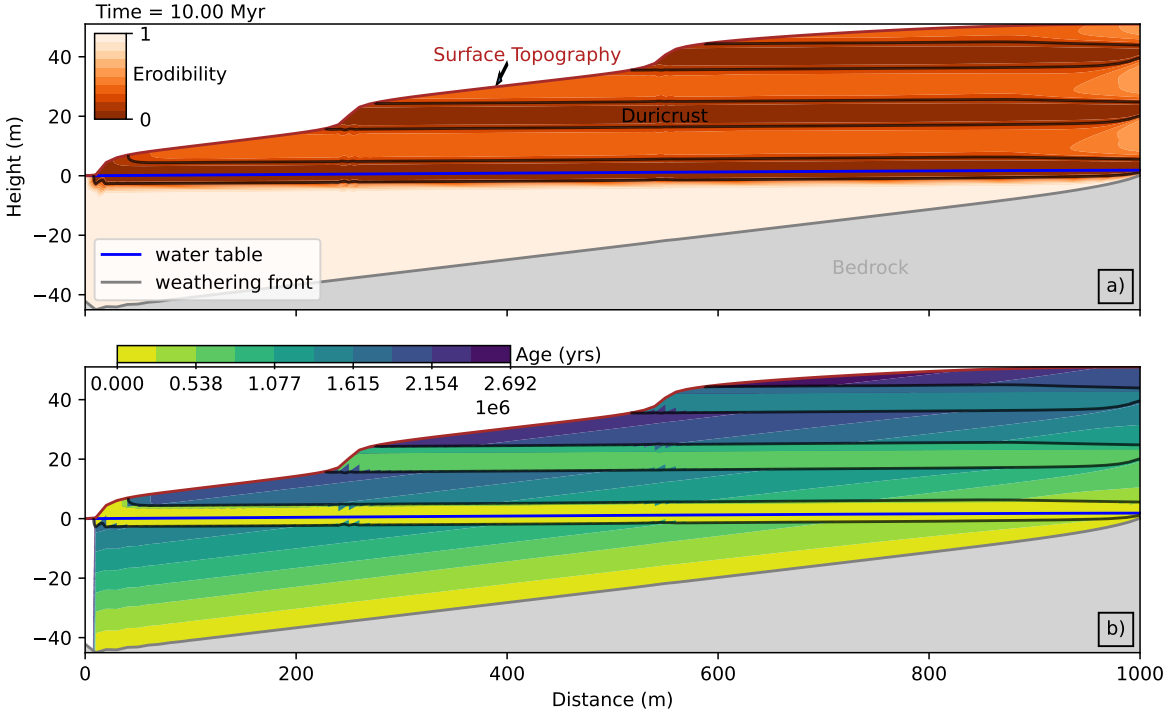

Figure 8. a) Model scenario with three iron duricrusts (outlined in black, dark red), formed in three different generations according to the equations given in figure 2.; b) Simulation of regolith and duricrust ages derived from the formation equations ruling the new model. The younger the age, the lighter the colour of the object. The older the age, the darker the colour of the object. Note that in the duricrust layers, the age corresponds to the age of the material when it passed through the water table; in the rest of the regolith, the age corresponds to the age of the material when it passed through the weathering front.

2.5 Dimensionless numbers and mapping of model behaviour

We now derive the basic conditions necessary for the formation of a ferricrete. Firstly, for a duricrust formed during the quiet period, the regolith material must spend sufficient time within the beating range of the water table, in comparison to the characteristic time scale for hardening, $\tau \times \frac{P}{P_{ref}}$. This leads to the definition of a first dimensionless number, that we will call W and define as:

$$W = \frac{\Phi}{\tau} \times \frac{P}{P_{ref}} \tag{8}$$

https://doi.org/10.5194/egusphere-2024-160
Preprint. Discussion started: 6 February 2024

Φ is here the duration of one of the cycles, but it must be understood in a more general context as the duration of the quiet period during which the regolith hardening takes place (regardless of the duration of the tectonic period). We see that if for a duricrust to form, W must be large.

Secondly, for a duricrust to form during an actively uplifting period, the same condition, i.e., that the time spent by the regolith within the beating range of the water table, in this case equal to $U \times \tau$, is equal or larger than the characteristic time scale for hardening, leads to the definition of another dimensionless number, which we called R_t:

$$R_t = \frac{\lambda}{U \times \tau} \times \frac{P}{P_{ref}} \tag{9}$$

And, again for ferricretes to form requires that R_t be large.

We note that the two numbers, W and R_t, are indeed dimensionless. To assess the exact range in the $[W - R_t]$ space over which iron duricrusts can form, we perform a large number of model experiments varying many of the model parameters simultaneously, including, λ, τ, U, Φ and P. The results are shown in figure 9a) where each of the 1296 model runs we performed has been represented by a coloured circle in the W-R_t space, where the colour is proportional to the logarithm of the maximum value of the erodability factor, κ, computed by the model and the duricrust formation threshold marked by κ_D. We see that the formation of a duricrust is favoured for high values of both W and R_t and that for the arbitrary threshold value of κ_D=0.2 as used in the above experiments, the conditions for duricrust formations are approximately:

$$W > 1 \quad \text{and} \quad R_t \geq 0.1 \tag{10}$$

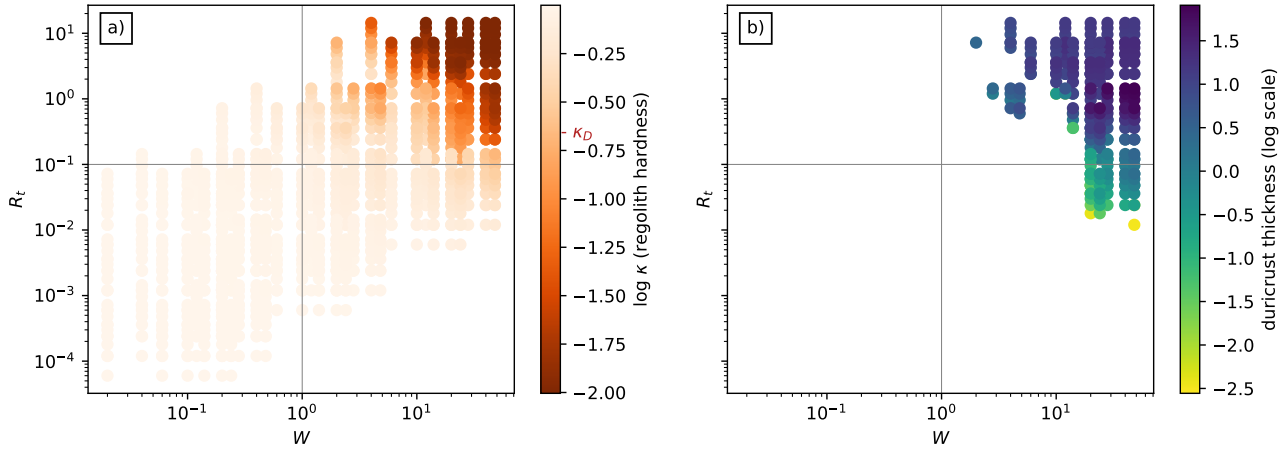

Figure 9. (a) Statistical study of 1296 scenarios illustrated in a log space scatter plot along dimensionless numbers R_t and W. Dots represent occurrence or not of iron duricrust formation according to the inputted parameters. Regolith hardness, or erodability, is represented through the colour scale: the lighter the colour, the softer the regolith, the darker the colour, the harder the regolith (creation of ferricretes). Formation conditions are met when approximately $R_t > 0.1$ and $W > 1$, according to the ferricrete formation threshold, defined by $\kappa_D = 0.2$ (in the top right space defined by the grey outlines); (b) Duricrust thickness illustrated in the same log space scatter plot. The lighter the colour, the thinner the ferricrete. The darker the colour, the thicker the ferricrete.

https://doi.org/10.5194/egusphere-2024-160
Preprint. Discussion started: 6 February 2024

In figure 9b), we show the duricrust thickness values computed from the same set of numerical experiments. We see that computed thicknesses are shown only above values for W and R_t approximately above 1 and 0.1, which also points to a duricrust formation threshold of $\kappa < \kappa_D$. Thicknesses range from centimetres to metres. The thinnest duricrusts are predominantly registered for lower R_t values, while the thickest values tend to be for high values of W and values of around 1 for R_t.

3 Discussion

3.1 Model behaviour

We have developed a model for the formation of duricrusts by lateral transport of ferrous ions and their precipitation in the beating range of the water table. Although based on sound physical and chemical processes, our model is purely parametric in that it depends on the values of heuristic parameters including the assumed range of seasonal variations in water table height, λ, and the characteristic time for precipitation of the hardening agent, τ, assumed to be inversely proportional to precipitation rate. This simple model reproduces the most widely accepted conditions for the formation of iron duricrusts: a wet, yet variable, climate in a relatively stable tectonic environment.

The model also shows that a period of uplift (or base level fall) is necessary to expose the duricrust to the surface. By modifying the surface erodability constant K_D (here the coefficient of transport on hill slopes) in proportion to the hardening parameter, κ, used to parameterise the progressive transformation of the regolith into hardened material, the model is able to reproduce the formation of one or several duricrusts that resist erosion and therefore protect the underlying regolith. According to our model, the age of formation of a duricrust can be equated to the time since the duricrust left the water table beating range. In figure 8b), we show computed ages for the model run shown in figure 8a). We see that regolith ages are always older than iron duricrust ages, and partially altered/hardened regolith is located above duricrusts and not below. This happens when the environment's activity changes and starts to uplift. If we observed inverted ages of duricrust generations, i.e. younger duricrusts on top of older ones, and altered regolith below duricrusts and not above, the recorded activity would not be characterized as uplift but rather as subsidence.

The absolute value of the hardening parameter is, however, arbitrary and determined by the ratio of the assumed characteristic time scale, τ and the duration of a period of tectonic quiescence. We hypothesise that a critical value of $\kappa = \kappa_D = 0.2$ corresponding to a decrease in surface erodability by a factor of 5 is such that it causes noticeable variations in topography that allow us to define the range of model parameters causing the formation of a duricrust as observed in the field.

3.2 Model parameters

The thickness of the duricrust depends strongly on the value of the parameter λ which indicates that the seasonality of rainfall and thus the beating range of the water table are the dominant factors that determine the thickness of the predicted duricrust. This correlates with observations in Africa (Tardy, 1993; Leduc et al., 1997), India (Sreedevi et al., 2006; Bhuiyan, 2010; Chandra et al., 2015; Kuruppath et al., 2018), Europe (Hassan et al., 2014; Balugani et al., 2017; Nygren et al., 2020), Asia

https://doi.org/10.5194/egusphere-2024-160
Preprint. Discussion started: 6 February 2024

(Moon et al., 2004; Deng et al., 2014) or Brazil (Allard et al., 2018). Depending on the region, long arid periods are observed with intensive fast wet seasons, sometimes monsoon driven, where duricrusts form that can attain up to 10 metres in thickness (Tardy et al., 1991; Tardy, 1993). On the other hand, where tropical, temperate or cold environments do not allow for important arid periods, duricrusts form, but are thinner (cms to a few ms). We note, also, that thicker duricrusts can be generated in the case of a very slow, yet continuous uplift (or base level fall) that would cause the water table to affect a much greater range of the regolith layer. As shown in figure 9b) duricrust thickness also varies according to the dimensionless parameters W and R_t. Duricrusts are the thickest for high values of W and R_t, but specifically more for values around 1 for R_t. Precipitation prone environments like tropical areas are located on the right side of figure 9. This result is highly interesting as it is in apparent contradiction with what we stated earlier, where the thickest duricrusts were created under semi-arid conditions as the water table fluctuation is highest in semi-arid areas (Leduc et al., 1997). Thus, dependence of duricrust thickness on λ may vary depending on external conditions. The water table beating range could be more prevalent under drier conditions, as our models show a correlation between λ and duricrust thickness as can be seen with figure 5, while other processes dictate duricrust thickness under tropical conditions. Tectonically active areas (low R_t values) are not prone to duricrust formation and when they do tend to create thinner crusts (lower part of figure 5).

As mentioned above, the value of the parameter τ is arbitrary. Constraining it by direct observations or the results of laboratory experiments on the kinetic of chemical reactions or the saturation in iron in the brine is difficult. Geochronological methods on iron oxides are a mean to provide approximate values for τ, through the range of ages that can be estimated on a single iron oxide nodule (Heller et al., 2022). This leads to postulate that a 'generic' value for τ could be in the range 50 - 1000 kyrs, although it is likely to be highly dependent on precipitation. Note that our model allows for a linear dependence of τ on precipitation, which we included in the model parametrisation by introducing a characteristic precipitation rate (taken to be 1 $m.yr^{-1}$) to which the specified value of τ corresponds.

3.3 Erosional time scale

During phases of tectonic activity or base-level fall, iron duricrust layers are uplifted from the water table height to the top of hills (figure 6). While being uplifted, we can see that the regolith layers as well as the duricrust layer are eroded with time, resulting in only a small patch of duricrust remaining at the top of the hill at the end of the uplift period (figure 6g)). When comparing duricrust hills with homogeneous regolith hills, we can see a difference in morphology and topographic height. However, as discussed earlier and shown in figure 7, there is almost no delay in erosion due to the presence of a duricrust, which seems contra-intuitive: if a hard layer protects soft rocks, it should take longer to erode the system. Many authors have previously described duricrusts in lateritic or regolith profiles (e.g. Tardy (1993); Taylor and Eggleton (2001)) as a protecting layer that should slow down erosion of the underlying topography/hill. We do not observe this in our model, and now proceed to explain it.

A hill containing a duricrust layer can be regarded as a layered material that is subjected to diffusion. The top and bottom layers have normal diffusivity, while the central layer has a diffusivity lowered by a factor κ. We ran a series of 1D diffusion model representing this situation, starting from an initially sinusoidal hill of arbitrary height and length but varying the position,

https://doi.org/10.5194/egusphere-2024-160
Preprint. Discussion started: 6 February 2024

thickness and hardness of the embedded horizontal layer. In Figure 10, we show the computed diffusive time, i.e., the time necessary for the hill maximum height to decrease by a factor e, normalized by the time it would take for a hill containing no duricrust, as a function of various parameters, i.e., the thickness of the duricrust layer, d, normalized by the hill height, its position p measured from the base of the hill and normalized by the hill height and the factor κ. We see that the diffusive time scale increases with the duricrust layer thickness and hardness (lower κ value). The dependence on the hardness is, however, very non-linear. The increase in the response time scale does not exceed a factor of 2, even for a reduction in diffusivity (or increase in hardness) of 100. This explains why a 'normal' duricrust, i.e., that represents only a few percent of a hill total thickness, does not strongly alter the erosional time scale of the hill, confirming the results previously presented in Figure 7. It also supports our arbitrary choice of a hardness factor of 0.2 (decrease in erodability by a factor 5) to define a duricrust layer.

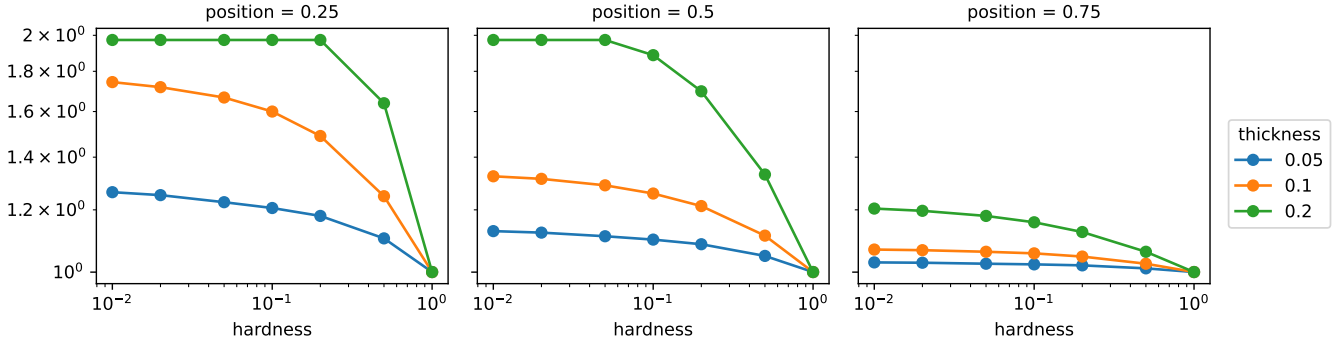

Figure 10. Increase in erosional time scale due to the presence of a duricrust, as a function of the assumed hardness of the duricrust (factor κ for three different values of the duricrust thickness (green, orange and blue lines) and three positions of the duricrust layer (from left to right). The position and thickness are relative to the hill height.

We also see that the position of the ferricrete has an effect on how it affects the erosional time scale of the hill. The closer it is to the base of the hill, the more it 'protects' the hill from being eroded. This results is interesting as it does not support the concept that duricrusts strongly protect topographic features over long geological time scales. They do, but not in proportion to their apparent strength: a duricrust that is 100 times harder than the surrounding hill can, at most (i.e. if it occupies 20% of the hill thickness), delay the erosion of the hill by a factor 2, even if it fills as much as 20% of the hill thickness. This may explain why, even though duricrusts are often found at the top of hills, suggesting that they 'protect' those hills, they are commonly found on a very small scale and are never preserved across very large scales. This therefore confirms the observation that ferricretes are very unstable layers and explains why they are often formed by re-cementing of fragments of previously collapsed duricrusts.

3.4 Important dimensionless numbers

We have shown that the model behaviour can be described in a dimensionless space containing two parameters, namely $R_t = \frac{\lambda}{U \times \tau} \times \frac{P}{P_{ref}}$ and $W = \frac{\Phi}{\tau} \times \frac{P}{P_{ref}}$. The first controls how long a section of the regolith layer stays in the vicinity of the water table

https://doi.org/10.5194/egusphere-2024-160
Preprint. Discussion started: 6 February 2024

while uplifting at a rate U and the other how long the material stays while not uplifting, in comparison to the characteristic time scale, τ. Both dimensionless numbers also incorporate the dependence of τ on mean precipitation rate. As expected, the region of this dimensionless parameter space that is conducive to duricrust formation corresponds to conditions of tectonic stability, as previously described by several authors such as Tardy (1993); Tardy and Roquin (1998); Vasconcelos and Conroy (2003); Taylor and Eggleton (2001) and high mean precipitation rate during a set, short, period of time, in agreement with the work of Tardy et al. (1991); Tardy (1993), which defines very detailed conditions for the creation of iron duricrusts, with annual mean precipitation of at least 1450 $mm.yr^{-1}$.

It is, however, worth noting that this region of parameter space corresponds also to conditions which, according to Braun et al. (2016), lead to the formation of a regolith layer that is thickest near its base level (or thins towards the top of the hill). As mentioned above, this corresponds to situations where the dimensionless number Γ is smaller than the ratio $\Omega^2/(\Omega-1)$. This point is highlighted in figure 11 where we show contours of the value of the ratio $\Gamma(\Omega-1)/\Omega^2$ (left column) and the maximum value of the hardening coefficient, κ, (right column) as a function of the assumed uplift rate, U_0 and precipitation rate, P_0, both assumed to be constant in space and time, for each of a range of $9 \times 9 \times 3 = 243$ experiments, in which those parameters were systematically varied across natural ranges. We see that for large values of τ, no duricrust form as the maximum value of $\log_{10}\kappa$ does not reach -0.7 ($= \log_{10}(0.2)$).

https://doi.org/10.5194/egusphere-2024-160
Preprint. Discussion started: 6 February 2024

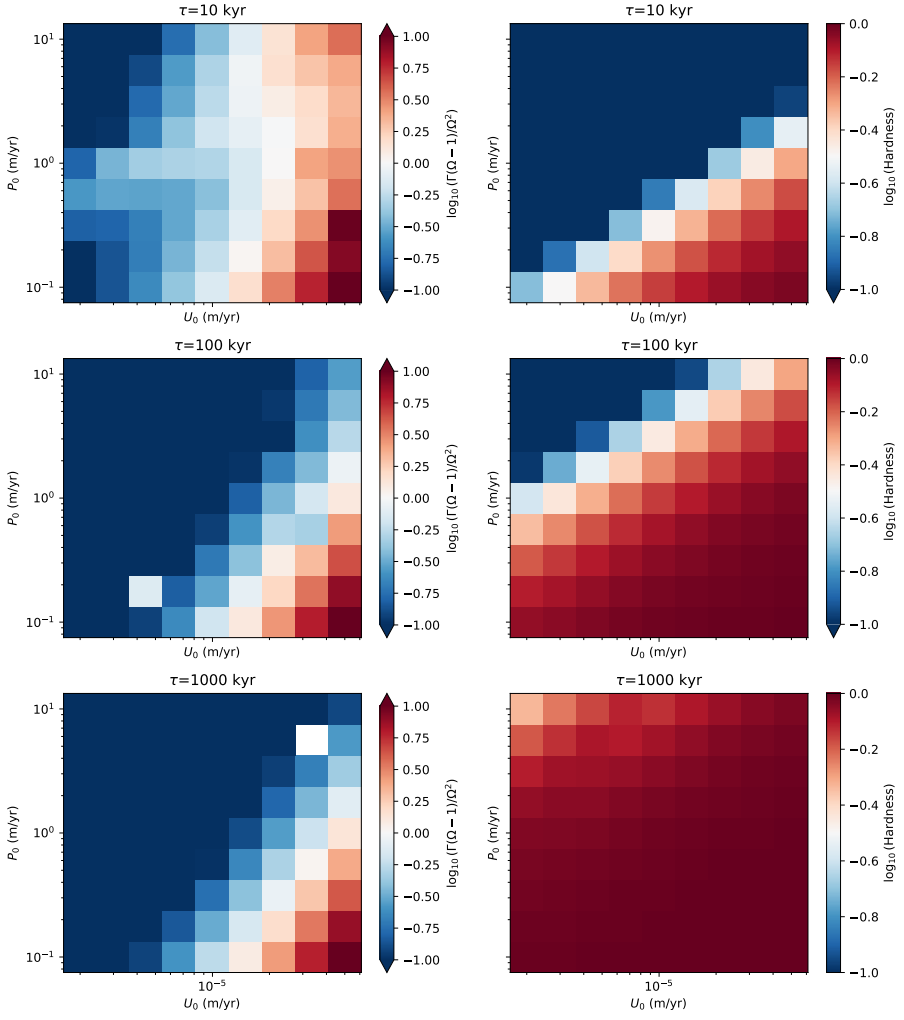

Figure 11. Left column: ratio $\Gamma(\Omega-1)/\Omega^2$ controlling the shape of the regolith layer (see Braun et al. (2016) for definition) as a function of the assumed uniform and constant uplift rate, U_0, and precipitation rate, P_0, for three values of the duricrust formation characteristic time scale, τ. Right column: contours of the maximum hardening coefficient, κ, for the same parameter values.

We note, however, that, for small values of τ, the simple pattern of the ratio $\Gamma(\Omega-1)/\Omega^2$ increasing with high uplift rate and low precipitation rate (leading to greater regolith thickness beneath the top of the hill than at its base level) is perturbed at mid-precipitation values. When a duricrust forms, it decreases the surface transport coefficient, which increases the surface slope. This, in turn, causes Ω to increase and Γ to increase. However, as Γ varies as the square of the slope, while Ω varies in direct proportion to the slope, the ratio $\Gamma(\Omega-1)/\Omega^2$ increases leading to the formation of a duricrust. Thus, the formation of a duricrust causes the regolith profile to thin near its base and to thicken towards the top of the hill. This feedback can be quite strong for low values of τ: compare the contours of $\Gamma(\Omega-1)/\Omega^2$ for $\tau = 10$ kyr (top left panel in figure 11) with those for $\tau = 1000$ kyr (bottom left panel in figure 11).

https://doi.org/10.5194/egusphere-2024-160
Preprint. Discussion started: 6 February 2024

3.5 Use ferricretes as markers for uplift

Most ore formation processes happen at the water table level. In some areas, research upon specific layers that are believed to have formed at base level and were uplifted, are used as markers and can tell us the uplift history of the region. However, as we have shown through the model, the water table is linked to a base level that does not need to be a continental-scale base level (i.e. the ocean). Therefore the position of an iron duricrust can only tell us about the uplift relative to this local base level. Thus, we cannot give an absolute uplift value if we do not have the uplifting or tectonic history of the region. One possible constrain with base level changes, would be the Quadrilatero Ferrifero region in Brazil. There, data from e.g. Spier et al. (2006); Monteiro et al. (2014, 2018); Vasconcelos and Conroy (2003); Vasconcelos and Carmo (2018) dated regolith and duricrust layers with which we will be able to propose a scenario of base level changes in the region. The values of all parameters will be defined with adequate values compared to the environment observed. As defined above, if the model parameters R_t and W are above ~0.1 and 1, duricrusts can form. This means that this model can be used without any environment dependence or areal restrictions.

A second possibility, depending on the mineralisation type, is that mineral formation takes place in the whole weathering profile and not just at the water table. In this case, determining a regional uplift through base level changes is not possible, as mineralisation is not a marker of a definite water table level. On the other hand, it is possible to define a weathering rate. The youngest ages registered are found at the weathering front, and mineralisations get older with decreasing depth in the weathering profile. This hypothesis contributes to the calibration of the minimum value of F in the numerical model's weathering process, but also opens future applications for new models based primarily on weathering.

3.6 Generalisation to other crusts

Other types of duricrusts form through hydrological processes (Taylor and Eggleton, 2001). One possible development and use of our model would consist in adjusting the value of the key rate parameter, i.e., τ , for each type of duricrusts, namely calcretes, silcretes or other types of hardened layers that are likely to form according to the hydrological model. It is known that different types of duricrusts form in different environments, most likely in an optimum moisture/climatic gradient in time and space (Webb and Nash, 2020; Taylor and Eggleton, 2001; Khalifa et al., 2009; Momo et al., 2020; Mather et al., 2019; Watson, 1988). Using the model, we could then map the tectonic and climatic scenarios under which each type of crust forms and explore potential differences in their long-term preservation. Another interesting perspective is the adaptation of this model to other supergene ore deposits. In Australia for example, deposits are considered to be in the regolith, which could be explained by a formation model such as the hydrological hypothesis for ferricretes.

4 Conclusions

We have developed a new model for the formation of duricrusts by adding a fourth component to an existing model for regolith formation by Braun et al. (2016) with the purpose of investigating how ferricritisation affects surface erosion and the potential feedback it has on regolith formation and evolution. It can also be seen as a first step towards validating the horizontal or

https://doi.org/10.5194/egusphere-2024-160
Preprint. Discussion started: 6 February 2024

hydrological duricrust formation hypothesis by investigating whether it can or cannot reproduce the major characteristics of iron duricrusts, including their aspect and geometry, but also the environments in which they are know to form.

Using the model, we have shown to which degree iron duricrust formation can alter surface topography but also the water table position and the regolith geometry through complex feedbacks. Braun et al. (2016) demonstrated the strong control that surface slope exerts on regolith geometry as well as uplift rate or base-level drop and precipitation rate. Some of these factors, namely uplift and precipitation rates, are also controls on duricrust formation but the main feedback arises from the control of duricrust formation on surface slope.

We demonstrated that, under the assumption that ferricrete formation is controlled by the dissolution, transport and precipitation of iron radicals from distant sources (the so-called horizontal or hydrological hypothesis) duricrusts preferentially form under quiet tectonic conditions. Furthermore the main control on duricrust thickness is the assumed water table beating range. For the duricrust to become exposed at the surface requires a phase of tectonic uplift (or base level fall) followed by denudation. So the most likely environment to produce a series of duricrust layers must involve a sequence of tectonic/uplift events punctuated by periods of tectonic stability.

Our parametrisation introduces two heuristic parameters that can be calibrated using independent constraints, although the range of possible values for the parameters are relatively large. Combining these parameters with those representing external forcings (precipitation rate and uplift rate), one can define two dimensionless coefficients, namely R_t and W, that can be used to map the conditions under which duricrust formation is most likely to take place. We have shown that when $W \geq 1$ and $R_t \geq 0.1$ approximately, iron duricrust formation is possible. Below these critical values, the conditions are usually not met.

We have shown that, although intrinsically very resistant to erosion, duricrusts are unlikely to protect landforms as commonly assumed. This is because of their relative low thickness in comparison to topographic relief. We have shown that it is not only the intrinsic strength (or resistance to erosion) and thickness that control how long a duricrust will resist erosion, and therefore protect a hill, but also the position of the duricrust with respect to the summit of the hill. Our prediction is consistent with the widespread observation that, when they are exhumed, duricrusts tend to be located near the summit of a hill but it does not support the concept that duricrusts protect the underlying relief over substantial amount of time. This will also explain why it is relatively rare to preserve extensive duricrust layers at the surface.

An important upgrade of the model would be to adapt parameters for different types of hydrologically forming duricrusts, e.g. calcretes and silcretes and different ore deposits. We could then investigate how they are affected by the same tectonic uplift scenario and, potentially and how they would differ in their preservation potential.

Another important development will be to generalize this model to two dimensions. This will enable a more realistic prediction of the extent and geometry of duricrusts and their surface expression, and, most likely simulate the formation of inverted topographies such as seen in southern regions of Australia.

However, the priority for us is now to develop a model that represents the competing formation hypothesis for duricrust formation, namely the laterisation or vertical hypothesis that will allow us to uncover the main differences in duricrust geometries and rate of formation predicted by the two models and, hopefully, determine which of the two hypotheses is most appropriate or, more likely, the conditions that will favor the formation of duricrust through one mechanism or the other.

https://doi.org/10.5194/egusphere-2024-160
Preprint. Discussion started: 6 February 2024

Code availability. Caroline Fenske. (2024). CarolineFenske/Duricrusts: Initial Release (v1.0). Zenodo. https://doi.org/10.5281/zenodo.10523101

Appendix A: Methods and Results

A1 Constraining new model parameters

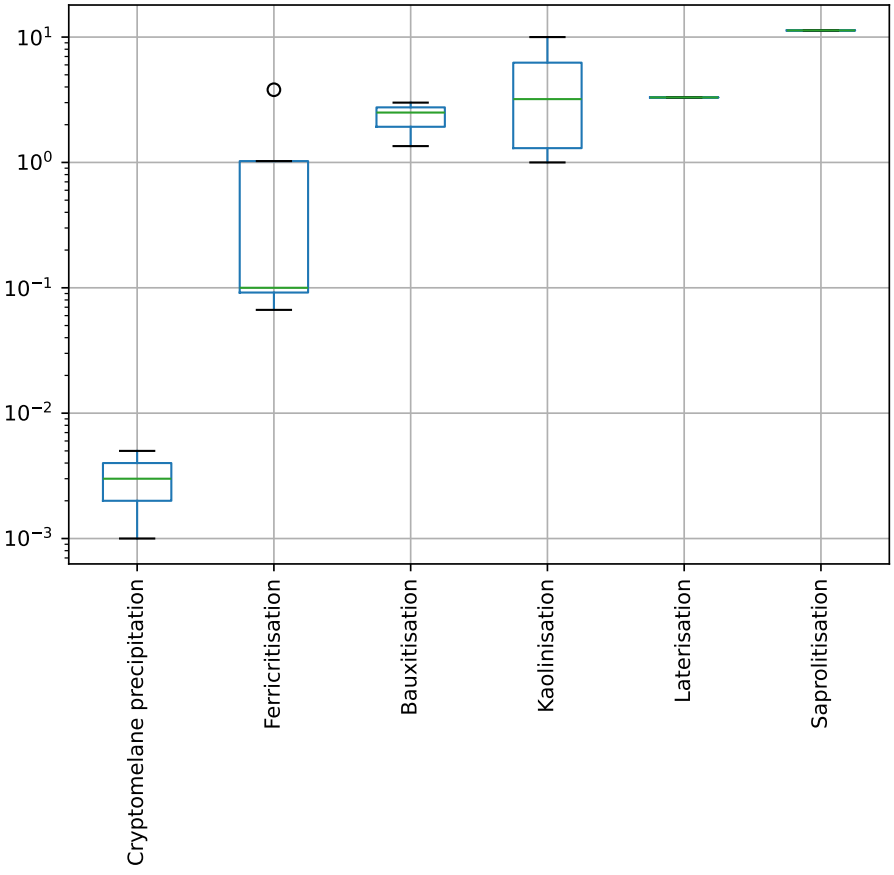

Figure A1. In this statistical box-plot representation, the green line represents the mean value, the blue box encompasses values from the lower quartile to the upper quartile, while the black whiskers limit at 1.5 of the interquartile range. The black circles represent outliers. Six different categories of weathering processes can be differentiated on the x-axis with their respective rates on the log y-axis as derived from literature. In this figure, only rates defined by authors in literature were plotted.

Author contributions. Caroline Fenske prepared the manuscript with contribution of Jean Braun, Cécile Robin and François Guillocheau. Caroline Fenske and Jean Braun developed the model, Caroline Fenske performed the simulations for the new model. François Guillocheau

https://doi.org/10.5194/egusphere-2024-160
Preprint. Discussion started: 6 February 2024

and Cécile Robin have given important contributions regarding the geochemistry, sedimentology and regolith knowledge, development of the idea of the main hypothesis.

Competing interests. No competing interests are present

590 *Acknowledgements.* The project has received funding from the European Union's Horizon 2020 research and innovation program under the Marie Sklodowska-Curie grant agreement No 860383.

https://doi.org/10.5194/egusphere-2024-160
Preprint. Discussion started: 6 February 2024

References

Achyuthan, H.: Paleopedology of ferricrete horizons around Chennai, Tamil Nadu, India, Revista mexicana de ciencias geológicas, ISSN 1026-8774, Vol. 21, Nº. 1, 2004 (Ejemplar dedicado a: VI International Symposium and Field Workshop on Paleopedology), pags. 133-143, 21, 910–917, https://doi.org/10.18203/2320-1770.ijrcog20230786, ferricrete soil needs from 1 to 6 Myrs Since at least Meso see fig 8 for some ages, 2004.

Allard, T., Gautheron, C., Riffel, S. B., Balan, E., Soares, B. F., Pinna-Jamme, R., Derycke, A., Morin, G., Bueno, G. T., and Nascimento, N. d.: Combined dating of goethites and kaolinites from ferruginous duricrusts. Deciphering the Late Neogene erosion history of Central Amazonia, Chemical Geology, 479, 136–150, https://doi.org/10.1016/j.chemgeo.2018.01.004, 2018.

Balugani, E., Lubczynski, M., Reyes-Acosta, L., Tol, C. v. d., Francés, A., and Metselaar, K.: Groundwater and unsaturated zone evaporation and transpiration in a semi-arid open woodland, Journal of Hydrology, 547, 54–66, https://doi.org/10.1016/j.jhydrol.2017.01.042, 2017.

Beauvais, A.: Ferricrete biochemical degradation on the rainforest–savannas boundary of Central African Republic, Geoderma, 150, 379–388, https://doi.org/10.1016/j.geoderma.2009.02.023, 2009.

Benedetti, M., Menard, O., and Noack, Y.: Geochemistry of water and chemical weathering rates under humid tropical climate, in: Water - Rock Interaction, pp. 545 – 548, A .A. Balkema, Rotterdam, 1992.

Bhuiyan, C.: Hydrogeological factors: their association and relationship with seasonal water-table fluctuation in the composite hardrock Aravalli terrain, India, Environmental Earth Sciences, 60, 733–748, https://doi.org/10.1007/s12665-009-0211-5, 2010.

Bonsor, H. C., MacDonald, A. M., and Davies, J.: Evidence for extreme variations in the permeability of laterite from a detailed analysis of well behaviour in Nigeria, Hydrological Processes, 28, 3563–3573, https://doi.org/10.1002/hyp.9871, wT in the lateritic profile (at 3m below surface, and laterite is 6 m deep) Hydro conductivity decreases with depth! water table seasonal fluctuation moste lat happening above K values, 2014.

Borger, H.: Mikromorphologie und Paläoenvironment: die Mineralverwitterung als Zeugnis der cretazisch-tertiären Umwelt in Süddeutschland, vol. 15, Gebrüder Borntraeger, 2000.

Boulangé, B.: Les formations bauxitiques latéritiques de Côte d'Ivoire : les faciès, leur transformation, leur distribution et l'évolution du modèle, Travaux et Documents de l'ORSTOM, ORSTOM, Paris, https://www.documentation.ird.fr/hor/fdi:15338, 1984.

Boulangé, B., Ambrosi, J.-P., and Nahon, D.: Laterites and Bauxites, in: Soils and Sediments Mineralogy and Geochemestry, edited by Springer, vol. 1, p. 369, Springer, https://doi.org/10.100/978-3-642-60525-3, 1997.

Bourman, R. P., Buckman, S., Chivas, A. R., Ollier, C. D., and Price, D. M.: Ferricretes at Burringurrah (Mount Augustus), Western Australia: Proof of lateral derivation, Geomorphology, 354, 107 017, https://doi.org/10.1016/j.geomorph.2019.107017, add to paper 1 as person talking about WT model!!!!, 2020.

Bovy, B., McBain, G. D., Gailleton, B., and Lange, R.: benbovy/xarray-simlab: 0.5.0, https://doi.org/10.5281/zenodo.4469813, 2021.

Brantley, S. L. and White, A. F.: Approaches to Modeling Weathered Regolith, Reviews in Mineralogy and Geochemistry, 70, 435–484, https://doi.org/10.2138/rmg.2009.70.10, 2009.

Brantley, S. L., Lebedeva, M. I., Balashov, V. N., Singha, K., Sullivan, P. L., and Stinchcomb, G.: Toward a conceptual model relating chemical reaction fronts to water flow paths in hills, Geomorphology, 277, 100–117, https://doi.org/10.1016/j.geomorph.2016.09.027, 2017.

Braun, J., Mercier, J., Guillocheau, F., and Robin, C.: A simple model for regolith formation by chemical weathering, Journal of Geophysical Research: Earth Surface, 121, 2140–2171, https://doi.org/10.1002/2016jf003914, 2016.

https://doi.org/10.5194/egusphere-2024-160
Preprint. Discussion started: 6 February 2024

Braun, J., Guillocheau, F., and Robin, C.: Reply to Comment on "A simple model for regolith formation by chemical weathering" by Braun et al. Contradictory concentrations and a tale of two velocities by Harman et al., Journal of Geophysical Research: Earth Surface, 122, 2037–2039, https://doi.org/10.1002/2017jf004271, 2017.

Campforts, B. and Govers, G.: Keeping the edge: A numerical method that avoids knickpoint smearing when solving the stream power law, Journal of Geophysical Research: Earth Surface, 120, 1189–1205, https://doi.org/10.1002/2014jf003376, 2015.

Campy, M. and Macaire, J.-J.: Altération météorique des roches, in: Géologie de la Surface - érosion, transfert et stockage dans les environnements continentaux, p. 448, Dunod, 2003.

Chandra, S., Singh, P. K., Tiwari, A. K., Panigrahy, B. P., and Kumar, A.: Evaluation of hydrogeological factors and their relationship with seasonal water table fluctuation in Dhanbad district, Jharkhand, India, ISH Journal of Hydraulic Engineering, 21, 193–206, https://doi.org/10.1080/09715010.2014.1002542, 2015.

Chardon, D.: Landform-regolith patterns of Northwestern Africa: Deciphering Cenozoic surface dynamics of the tropical cratonic geosystem, Earth-Science Reviews, 242, 104 452, https://doi.org/10.1016/j.earscirev.2023.104452, canga = specific ferricrete formed on top of BIFS, 2023.

Chivas, A. R. and Atlhopheng, J. R.: Oxygen-isotope dating the Yilgarn regolith, Geological Society, London, Special Publications, 346, 309–320, https://doi.org/10.1144/sp346.16, 2010.

Deng, Y., Li, H., Wang, Y., Duan, Y., and Gan, Y.: Temporal Variability of Groundwater Chemistry and Relationship with Water-table Fluctuation in the Jianghan Plain, Central China, Procedia Earth and Planetary Science, 10, 100–103, https://doi.org/10.1016/j.proeps.2014.08.018, 2014.

dos Santos Albuquerque, M. F., Horbe, A. M. C., and Danišík, M.: Episodic weathering in Southwestern Amazonia based on (UTh)/He dating of Fe and Mn lateritic duricrust, Chemical Geology, 553, 119 792, https://doi.org/10.1016/j.chemgeo.2020.119792, 2020.

Ely, D. M. and Kahle, S. C.: Simulation of groundwater and surface-water resources and evaluation of water-management alternatives for the Chamokane Creek basin, Stevens County, Washington, Tech. Rep. 2012-5224, USGS, 10.3133/sir20125224, 2012.

Ferrier, K. L. and Kirchner, J. W.: Effects of physical erosion on chemical denudation rates: A numerical modeling study of soil-mantled hillslopes, Earth and Planetary Science Letters, 272, 591–599, https://doi.org/10.1016/j.epsl.2008.05.024, 2008.

Fritz, B. and Tardy, Y.: Etude thermodynamique du système gibbsite, quartz, kaolinite, gaz carbonique. Application à la genèse des podzols et des bauxites, Sciences Géologiques. Bulletin, 26, 339–367, https://doi.org/10.3406/sgeol.1973.1438, 1973.

Gac, J.-Y.: Géochimie du bassin du lac Tchad : Bilan de l'altération de l'érosion et de la sédimentation, Ph.D. thesis, ORSTOM, https://www.documentation.ird.fr/hor/fdi:00039, 1980.

Girard, J.-P., Freyssinet, P., and Morillon, A.-C.: Oxygen isotope study of Cayenne duricrust paleosurfaces: implications for past climate and laterization processes over French Guiana, Chemical Geology, 191, 329–343, https://doi.org/10.1016/s0009-2541(02)00130-4, 2002.

Guinoiseau, D., Fekiacova, Z., Allard, T., Druhan, J. L., Balan, E., and Bouchez, J.: Tropical Weathering History Recorded in the Silicon Isotopes of Lateritic Weathering Profiles, Geophysical Research Letters, 48, https://doi.org/10.1029/2021gl092957, 2021.

Hassan, S. T., Lubczynski, M. W., Niswonger, R. G., and Su, Z.: Surface–groundwater interactions in hard rocks in Sardon Catchment of western Spain: An integrated modeling approach, Journal of Hydrology, 517, 390–410, https://doi.org/10.1016/j.jhydrol.2014.05.026, 2014.

Heller, B. M., Riffel, S. B., Allard, T., Morin, G., Roig, J.-Y., Couëffé, R., Aertgeerts, G., Derycke, A., Ansart, C., Pinna-Jamme, R., and Gautheron, C.: Reading the climate signals hidden in bauxite, Geochimica et Cosmochimica Acta, 323, 40–73, https://doi.org/10.1016/j.gca.2022.02.017, 2022.

https://doi.org/10.5194/egusphere-2024-160
Preprint. Discussion started: 6 February 2024

Horbe, A. M. C. and Anand, R.: Bauxite on igneous rocks from Amazonia and Southwestern of Australia: Implication for weathering process, Journal of Geochemical Exploration, 111, 1–12, https://doi.org/10.1016/j.gexplo.2011.06.003, 2011.

Hénocque, O., Ruffet, G., Colin, F., and Féraud, G.: 40Ar/39Ar dating of West African lateritic cryptomelanes, Geochimica et Cosmochimica Acta, 62, 2739–2756, https://doi.org/10.1016/s0016-7037(98)00185-9, manganese duri, 1998.

Khalifa, M., Kumon, F., and Yoshida, K.: Calcareous duricrust, Al Qasim Province, Saudi Arabia: Occurrence and origin, Quaternary International, 209, 163–174, https://doi.org/10.1016/j.quaint.2009.02.014, 2009.

Kuruppath, N., Raviraj, A., Kannan, B., and Sellamuthu, K. M.: Estimation of Groundwater Recharge Using Water Table Fluctuation Method, International Journal of Current Microbiology and Applied Sciences, 7, 3404–3412, https://doi.org/10.20546/ijcmas.2018.710.395, 2018.

Lebedeva, M. and Brantley, S.: A clarification and extension of our model of regolith formation on hillslopes, Earth Surface Processes and Landforms, 43, 2715–2723, https://doi.org/10.1002/esp.4426, 2018.

Lebedeva, M., Fletcher, R., Balashov, V., and Brantley, S.: A reactive diffusion model describing transformation of bedrock to saprolite, Chemical Geology, 244, 624–645, https://doi.org/10.1016/j.chemgeo.2007.07.008, 2007.

Lebedeva, M., Fletcher, R., and Brantley, S.: A mathematical model for steady-state regolith production at constant erosion rate, Earth Surface Processes and Landforms, 35, 508–524, https://doi.org/10.1002/esp.1954, 2010.

Lebedeva, M. I. and Brantley, S. L.: Exploring geochemical controls on weathering and erosion of convex hillslopes: beyond the empirical regolith production function, Earth Surface Processes and Landforms, 38, 1793–1807, https://doi.org/10.1002/esp.3424, 2013.

Leduc, C., Bromley, J., and Schroeter, P.: Water table fluctuation and recharge in semi-arid climate: some results of the HAPEX-Sahel hydrodynamic survey (Niger), Journal of Hydrology, 188, 123–138, https://doi.org/10.1016/s0022-1694(96)03156-3, 1997.

Leer, B. v.: Towards the ultimate conservative difference scheme. II. Monotonicity and conservation combined in a second-order scheme, Journal of Computational Physics, 14, 361–370, https://doi.org/10.1016/0021-9991(74)90019-9, 1974.

Leneuf, N.: L'altération des granites calco-alcalins et des granodiorites en Côte d'Ivoire forestière et les sols qui en sont dérivés, Ph.D. thesis, Université de Paris ; ORSTOM, Paris (FRA) ; Paris, 1959.

Maher, K.: The dependence of chemical weathering rates on fluid residence time, Earth and Planetary Science Letters, 294, 101–110, https://doi.org/10.1016/j.epsl.2010.03.010, 2010.

Marques, E. A., Junior, G. C. S., Eger, G. Z., Ilambwetsi, A. M., Raphael, P., Generoso, T. N., Oliveira, J., and Júnior, J. N.: Analysis of groundwater and river stage fluctuations and their relationship with water use and climate variation effects on Alto Grande watershed, Northeastern Brazil, Journal of South American Earth Sciences, 103, 102 723, https://doi.org/10.1016/j.jsames.2020.102723, 2020.

Maréchal, J., Dewandel, B., Ahmed, S., Galeazzi, L., and Zaidi, F.: Combined estimation of specific yield and natural recharge in a semi-arid groundwater basin with irrigated agriculture, Journal of Hydrology, 329, 281–293, https://doi.org/10.1016/j.jhydrol.2006.02.022, 2006.

Mather, C. C., Nash, D. J., Dogramaci, S., Grierson, P. F., and Skrzypek, G.: Geomorphic and hydrological controls on groundwater dolocrete formation in the semi-arid Hamersley Basin, northwest Australia, Earth Surface Processes and Landforms, 44, 2752–2770, https://doi.org/10.1002/esp.4704, 2019.

Momo, M. N., Beauvais, A., Tematio, P., and Yemefack, M.: Differentiated Neogene bauxitization of volcanic rocks (western Cameroon): Morpho-geological constraints on chemical erosion, CATENA, 194, 104 685, https://doi.org/10.1016/j.catena.2020.104685, 2020.

Monteiro, H. S., Vasconcelos, P. M., Farley, K. A., Spier, C. A., and Mello, C. L.: (U–Th)/He geochronology of goethite and the origin and evolution of cangas, Geochimica et Cosmochimica Acta, 131, 267–289, https://doi.org/10.1016/j.gca.2014.01.036, 2014.

https://doi.org/10.5194/egusphere-2024-160
Preprint. Discussion started: 6 February 2024

Monteiro, H. S., Vasconcelos, P. M. P., and Farley, K. A.: A Combined (U-Th)/He and Cosmogenic 3He Record of Landscape Armoring by Biogeochemical Iron Cycling, Journal of Geophysical Research: Earth Surface, 123, 298–323, https://doi.org/10.1002/2017jf004282, 2018.

Moon, S.-K., Woo, N. C., and Lee, K. S.: Statistical analysis of hydrographs and water-table fluctuation to estimate groundwater recharge, Journal of Hydrology, 292, 198–209, https://doi.org/10.1016/j.jhydrol.2003.12.030, 2004.

Nahon, D.: Introduction to the petrology of soils and chemical weathering, vol. 1, John Wiley & Sons, 1991.

Nahon, D. and Bocquier, G.: Petrology of elements transfers in weathering and soil systems, in: Pétrologie des altérations et des sols. Vol. II : Pétrologie des séquences naturelles. Colloque international du CNRS, Paris 4-7 juillet 1983., Sciences Géologiques, bulletins et mémoires, https://www.persee.fr/doc/sgeol_0302-2684_1983_act_72_1_2016, included in a thematic issue : Pétrologie des altérations et des sols. Vol. II : Pétrologie des séquences naturelles. Colloque international du CNRS, Paris 4-7 juillet 1983., 1983.

Nash, D. J., Shaw, P. A., and Thomas, D. S. G.: Duricrust development and valley evolution: Process–landform links in the kalahari, Earth Surface Processes and Landforms, 19, 299–317, https://doi.org/10.1002/esp.3290190403, 1994.

Norton, K. P., Molnar, P., and Schlunegger, F.: The role of climate-driven chemical weathering on soil production, Geomorphology, 204, 510–517, https://doi.org/10.1016/j.geomorph.2013.08.030, 2014.

Nygren, M., Giese, M., Kløve, B., Haaf, E., Rossi, P. M., and Barthel, R.: Changes in seasonality of groundwater level fluctuations in a temperate-cold climate transition zone, Journal of Hydrology X, 8, 100 062, https://doi.org/10.1016/j.hydroa.2020.100062, 2020.

Ollier, C. and Galloway, R.: The laterite profile, ferricrete and unconformity, CATENA, 17, 97–109, https://doi.org/10.1016/0341-8162(90)90001-t, 1990.

Ollier, C. D. and Sheth, H. C.: The High Deccan duricrusts of India and their significance for the 'laterite' issue, Journal of Earth System Science, 117, 537, https://doi.org/10.1007/s12040-008-0051-9, 2008.

Paquet, H. and Clauer, N.: Soils and Sediments, Mineralogy and Geochemistry, Springer, https://doi.org/10.1007/978-3-642-60525-3, 1997.

Paton, T. R. and Williams, M. A. J.: The Concept of Laterite, Annals of the Association of American Geographers, 62, 42–56, https://doi.org/10.1111/j.1467-8306.1972.tb00842.x, 1972.

Pelletier, J. D.: How do pediments form?: A numerical modeling investigation with comparison to pediments in southern Arizona, USA, GSA Bulletin, 122, 1815–1829, https://doi.org/10.1130/b30128.1, 2010.

Pelletier, J. D., Broxton, P. D., Hazenberg, P., Zeng, X., Troch, P. A., Niu, G., Williams, Z., Brunke, M. A., and Gochis, D.: A gridded global data set of soil, intact regolith, and sedimentary deposit thicknesses for regional and global land surface modeling, Journal of Advances in Modeling Earth Systems, 8, 41–65, https://doi.org/10.1002/2015ms000526, 2016.

Retallack, G. J.: Soils of the Past, Blackwell Science, USA, https://doi.org/10.1002/9780470698716, 2001.

Retallack, G. J.: Lateritization and Bauxitization Events, Economic Geology, 105, 655–667, https://doi.org/10.2113/gsecongeo.105.3.655, 2010.

Ricordel-Prognon, C., Lagroix, F., Moreau, M., and Thiry, M.: Lateritic paleoweathering profiles in French Massif Central: Paleomagnetic datings, Journal of Geophysical Research: Solid Earth (1978–2012), 115, https://doi.org/10.1029/2010jb007419, 2010.

Riffel, S. B., Vasconcelos, P. M., Carmo, I. O., and Farley, K. A.: Goethite (U–Th)/He geochronology and precipitation mechanisms during weathering of basalts, Chemical Geology, 446, 18–32, https://doi.org/10.1016/j.chemgeo.2016.03.033, (U–Th)/He geochronology on goethite Mars analogy no duricrusts in the observed sites, more like ferruginzed layers fe layers in-between soil and saporolite. Weathering from "above", percolating waters. Duri formation just below surface WT hypothesis candidate? YES, see 4.1.1. Fig.7 histogram of goethite ages, 2016.

https://doi.org/10.5194/egusphere-2024-160
Preprint. Discussion started: 6 February 2024

Sacek, V., Neto, J. M. M., Vasconcelos, P. M., and Carmo, I. O.: Numerical Modeling of Weathering, Erosion, Sedimentation, and Uplift in a Triple Junction Divergent Margin, Geochemistry, Geophysics, Geosystems, 20, 2334–2354, https://doi.org/10.1029/2018gc008124, 2019.

Spier, C. A., Vasconcelos, P. M., and Oliviera, S. M.: 40Ar/39Ar geochronological constraints on the evolution of lateritic iron deposits in the Quadrilátero Ferrífero, Minas Gerais, Brazil, Chemical Geology, 234, 79–104, https://doi.org/10.1016/j.chemgeo.2006.04.006, 2006.

Sreedevi, P. D., Ahmed, S., Made, B., Ledoux, E., and Gandolfi, J. M.: Association of hydrogeological factors in temporal variations of fluoride concentration in a crystalline aquifer in India, Environmental Geology, 50, 1–11, https://doi.org/10.1007/s00254-005-0167-z, 2006.

Strasser, M., Strasser, A., Pelz, K., and Seyfried, H.: A mid Miocene to early Pleistocene multi-level cave as a gauge for tectonic uplift of the Swabian Alb (Southwest Germany), Geomorphology, 106, 130–141, https://doi.org/10.1016/j.geomorph.2008.09.012, 2009.

Tardy, Y.: Géochimie des altérations. Étude des arènes et des eaux de quelques massifs cristallins d'Europe et d'Afrique, Sciences Géologiques, bulletins et mémoires, CNRS, https://www.persee.fr/doc/sgeol_0080-9020_1969_mon_31_1, 1969.

Tardy, Y.: Silice, silicates magnésiens, silicates sodiques et géochimie des paysages arides, Bulletin de la Société géologique de France, XXIII, 325 – 334, 1981.

Tardy, Y.: Cuirasses latéritiques et minéralisations aurifères de la région de Kangaba au Mali., Cartographie, minéralogie, géochimie et télédetection, ORSTOM, DNGM, CNRS, rapport de Première Phase, 1986.

Tardy, Y.: Pétrologie des latérites et des sols tropicaux, vol. 1, Masson, 1993.

Tardy, Y. and Roquin, C.: Dérive des continents, Paléoclimats et altérations tropicales, vol. 1, BRGM, 1998.

Tardy, Y. and Roquin, R.: Geochemistry and evolution of lateritic landscapes, in: Weathering, soils and paleosols, Elsevier, title of the book: Weathering, soils and paleosols Chapter 16, 1992.

Tardy, Y., Bardossy, G., and Nahon, D.: Fluctuations de l'activité de l'eau et succesions de minéraux hydratés et déshydratés au sein des profils latéritiques ferrugineux et bauxitiques, C. R. Académie des Sciences de Paris, 307, 753 – 759, 1988.

Tardy, Y., Kobilsek, B., and Paquet, H.: Mineralogical composition and geographical distribution of African and Brazilian periatlantic laterites. The influence of continental drift and tropical paleoclimates during the past 150 million years and implications for India and Australia, Journal of African Earth Sciences (and the Middle East), 12, 283–295, https://doi.org/10.1016/0899-5362(91)90077-c, 1991.

Taylor, G. and Eggleton, R. A.: Regolith Geology and Geomorphology, Wiley, 1 edn., https://www.wiley.com/en-fr/Regolith+Geology+and+Geomorphology-p-9780471974543, 2001.

Temgoua, E., Tchapnga, H. D., Tanawa, E., Guenat, C., and Pfeifer, H.: Groundwater fluctuations and footslope ferricrete soils in the humid tropical zone of southern Cameroon, Hydrological Processes, 19, 3097–3111, https://doi.org/10.1002/hyp.5834, fig 6 WTF of about 2 meters in semi arid area with non monsoon pattern, so no extremes!, 2005.

Théveniaut, H. and Freyssinet, P.: Paleomagnetism applied to lateritic profiles to assess saprolite and duricrust formation processes: the example of Mont Baduel profile (French Guiana), Palaeogeography, Palaeoclimatology, Palaeoecology, 148, 209–231, https://doi.org/10.1016/s0031-0182(98)00183-7, 1999.

Théveniaut, H. and Freyssinet, P.: Timing of lateritization on the Guiana Shield: synthesis of paleomagnetic results from French Guiana and Suriname, Palaeogeography, Palaeoclimatology, Palaeoecology, 178, 91–117, https://doi.org/10.1016/s0031-0182(01)00404-7, 2002.

Théveniaut, H., Quesnel, F., Wyns, R., and Hugues, G.: Palaeomagnetic dating of the "Borne de Fer" ferricrete (NE France): Lower Cretaceous continental weathering, Palaeogeography, Palaeoclimatology, Palaeoecology, 253, 271–279, https://doi.org/10.1016/j.palaeo.2007.01.010, 2007.

https://doi.org/10.5194/egusphere-2024-160
Preprint. Discussion started: 6 February 2024

Vasconcelos, P. M. and Carmo, I. d. O.: Calibrating denudation chronology through 40Ar/39Ar weathering geochronology, Earth-Science Reviews, 179, 411–435, https://doi.org/10.1016/j.earscirev.2018.01.003, 2018.

Vasconcelos, P. M. and Conroy, M.: Geochronology of weathering and landscape evolution, Dugald River valley, NW Queensland, Australia, Geochimica et Cosmochimica Acta, 67, 2913–2930, https://doi.org/10.1016/s0016-7037(02)01372-8, 2003.

Vasconcelos, P. M., Becker, T. A., Renne, P. R., and Brimhall, G. H.: Age and Duration of Weathering by 40K-40Ar and 40Ar/39Ar Analysis of Potassium-Manganese Oxides, Science, 258, 451–455, https://doi.org/10.1126/science.258.5081.451, 1992.

Watson, A.: Desert gypsum crusts as palaeoenvironmental indicators: A micropetrographic study of crusts from southern Tunisia and the central Namib Desert, Journal of Arid Environments, 15, 19–42, https://doi.org/10.1016/s0140-1963(18)31002-4, 1988.

Webb, J. A. and Nash, D. J.: Reassessing southern African silcrete geochemistry: implications for silcrete origin and sourcing of silcrete artefacts, Earth Surface Processes and Landforms, 45, 3396–3413, https://doi.org/10.1002/esp.4976, 2020.

Wells, M., Danišík, M., McInnes, B., and Morris, P.: (U-Th)/He-dating of ferruginous duricrust: Insight into laterite formation at Boddington, WA, Chemical Geology, 522, 148–161, https://doi.org/10.1016/j.chemgeo.2019.05.030, 2019.

Widdowson, M.: Natural Resources of Goa, Natural Resources of Goa: A Geological Perspective, https://doi.org/978-81-908737-0-3, 2009.